THESIS

This is to certify that the

thesis entitled

EFFECT OF AN OIL FOG UPON

HOT-WIRE ANEMOMETRY RESPONSE

presented by

Wendelin Michael Burkhardt

has been accepted towards fulfillment
of the requirements for

Master of Science degree in Mechanical Engineering

R E Kaiser

Major professor

Date March 31,1982

EFFECT OF AN OIL FOG UPON HOT-WIRE ANEMOMETRY RESPONSE

By

Wendelin Michael Burkhardt

A THESIS

Submitted to
Michigan State University
in partial fulfillment of the requirements
for the degree of

MASTER OF SCIENCE

Department of Mechanical Engineering

1982

ABSTRACT

EFFECT OF AN OIL FOG UPON HOT-WIRE ANEMOMETRY RESPONSE

by

Wendelin Michael Burkhardt

In recent years, the use of flow visualization techniques have qualitatively revealed considerable insight into the nature of turbulent flows. Due to the difficulty of obtaining quantitative data from photographs, flow visualization techniques are being used in conjunction with classical anemometry techniques. This report addresses the effect one type of flow visualization tracer, namely an oil fog, has upon the response characteristics of a hot-wire anemometer. The study examined the effects of varying sensor temperature, oil fog concentration, air velocity and probe geometry. The relative errors of hot-wire mean velocity, fluctuating velocity and spectral measurements are also investigated. At the highest sensor operating temperature examined, corresponding to a resistance ratio of 1.8, the hot-wire performance was effected very little by the oil fog concentrations used. This was not the case at lower resistance ratios. Hot-wire voltage-velocity calibrations showed the Collis and Williams relationship held for all resistance ratios and oil fog concentration levels tested.

Finally, a model is proposed to explain the behavior of a hot-wire in an oil fog.

I dedicate this manuscript to my wife Kim. For her love and understanding aided immeasurably in its completion.

ACKNOWLEDGEMENTS

I wish to express my sincere thanks to Professor Robert E. Falco for his helpful advice and discussions during the course of this work.

The research ran over the course of 5 years and funds were supplied jointly by Air Force Office of Scientific Research under Contract #AFOSR-78-3703, monitored initially be Colonel Lowell Ormand and subsequently by Captain Michael Francis, and by the Office of Naval Research under contract #N0001477C0348, monitored initially by Ralph Cooper and subsequently by Robert Whitehead.

Table of Contents

List of Figures

List of Figures - Continued

List of Tables

List of Symbols

a	extinction coefficient per unit volume
A_{EX}	droplet specific projected extinction area
b	angle between hot-wire sensor and oncoming flow velocity vector, ambient pressure
C	non dimensional oil fog concentration
d	diameter
E	hot-wire anemometer output voltage
E_o	constant in hot-wire heat transfer law
E_{RMS}	hot-wire root-mean-square voltage
$E_{RMS_{CA}}$	hot-wire root-mean-square voltage in clean air
$E_{RMS_{OF}}$	hot-wire root-mean-square voltage in oil fog
F	force, coefficient of determination
h	convection heat transfer coefficient
I	intensity
I_o	initial intensity
k	constant in hot-wire heat transfer law
K	conduction heat transfer coefficient
L	length
m	constant in hot-wire heat transfer law complex index of refraction
M	momentum
M_c	droplet mass concentration
P	pressure
q	heat transfer
R	hot-wire resistance ratio
r_i	inner radius
r_o	outer radius
t	time
T	temperature
v	velocity
V	volume
σ	surface tension, standard deviation

CHAPTER 1
INTRODUCTION

1.1 Introduction

In recent years, flow visualization has developed into a very important tool with which to study coherent motions in turbulent flows. The types of flow visualization methods in use today are quite varied. Many visualization techniques seed the fluid being studied with a tracer that will follow the motions of the fluid. The type of tracer used depends upon the working medium. Typically solid particulates and gas bubbles are used in liquids while solid particulates and liquid droplets are used in air.

The technique of flow visualization allows researchers to observe the instantaneous flow field associated with short-lived coherent structures. With conventional flow visualization techniques, velocity records are very difficult, if not impossible, to obtain. This has lead to a new technique which combines the flow visulization method used by Fiedler and Head (1966) with simultaneous hot-wire anemometry, Falco (1977, 1980). A fog of 5 μm mineral oil droplets is illuminated by a thin sheet of laser light. The hot-wire sensors are placed in the laser light plane and a motion picture is taken of both the flow and the hot-wire anemometer output. In later measurements, Falco (1980) used laser light and simultaneous digital data acquisition to allow more accurate and rapid analysis to be made. Use of this technique to conditionally sample velocity records will yield a wealth of new and important information about the importance of coherent structures in turbulent flows.

This study was initiated to determine the effect the oil fog has on a hot-wire anemometer's response characteristics.

1.2 Hot-Wire Anemometers

The operation of a constant temperature hot-wire anemometer in air is quite well documented, so only a brief explanation of its operation will be given. The hot-wire operates by heating a thin wire to a temperature well above the ambient air temperature with an electric current and then maintaining this temperature constant throughout the period of operation. This operation is performed by the electronics maintaining the resistance of the hot-wire sensing element constant. If the sensor is then placed in a moving airstream, thermal convection will remove energy from the wire. By varying the current passing through the wire, the energy supplied to the wire is varied to maintain the temperature constant.

The basic electronic circuit used for constant temperature hot-wire anemometers is the Wheatstone bridge. In this circuit, Figure 1.1, the resistance of the hot-wire is held constant by varying resistance R_4. This varies the current that passes through the hot-wire. As the current through the hot-wire varies, so must the voltage drop across the wire. By calibrating this voltage against an air velocity, a functional relationship can be obtained between the two quantities.

A considerable amount of research has been performed to yield the current understanding of the operation of hot-wires in air. King (1914) first obtained the result that hot-wires obey a heat-transfer law of the form

$$E^2 = E_0{}^2 + kV^{1/2}$$

This relationship was later more closely examined by Collis and Williams(1959). They found that hot-wires, operated normal to the oncoming velocity vector, tend to behave according to the law

$$E^2 = E_0^2 + kV^m$$

where m may vary from 0.35 to 0.5 depending upon the individual hot-wire.

For operational reasons, it is desirable to operate a hot-wire not only normal to the air velocity vector, but also at other angles. A single hot-wire, positioned normal to the oncoming velocity vector, can only resolve the streamwise velocity component. This probe arrangement is typically called a u-wire because in a wind tunnel, the streamwise or u velocity component, is measured with this type of probe arrangement. To resolve two velocity components of the air flow requires the use of two hot-wire sensors, neither of which is normal to the oncoming velocity vector. These types of probes have the hot-wire sensors positioned at approximately 45° to the mean velocity vector and the wire axes orthogonal to one another. The resultant arrangement is typically termed an X-wire or V-wire array, depending upon the probe arrangement. The spatial separation of the two wires is typically 1 mm.

To allow the use of the Collis and Williams relationship on a probe that is not normal to the oncoming flow vector, the angle between the hot-wire axis and the flow must be considered. Friehe and Schwartz (1969) proposed the replacing the actual fluid velocity with an effective velocity calculated from the equation.

$$V_{EFF} = V_{ACT} \{1-.92[1-COS^{1/2}\beta]\}^2$$

Because of the relative ease of use and documented favorable response characteristics to high frequency flow fluctuations, hot-wires have been used for velocity measurements in many types of fluid media. This widespread use has demonstrated that hot-wire response can easily be effected by contaminants on the hot-wire. It is known that when hot-

wires are operated in media containing dirt and other contaminants voltage drifts occur. Morrow and Kline (1974) investigated the effects of operating a hot-wire anemometer in dirty water. They concluded the dirt formed a coating on the sensor which resulted in increased heat transfer resistance. The size of the coating would increase in time. This would cause the parameters of the Collis and Williams relationship to change with time. Morrow and Kline also noted that the energy spectra showed considerably more noise at high frequencies.

The more subtle changes in the hot-wire's response when operated in a fog of mineral oil droplets, also termed "smoke", have also been examined. Investigations by Falco and Abell (unpublished) and Falco and Sniegowski (unpublished) have been performed using a similar oil fog as in this investigation. Falco and Abell found hot-wires were effected but slightly by the oil fog for resistance ratios of 1.6 and greater. The mean and rms voltage measurements made showed an increase in both quantities. Falco and Abell concluded a coating of oil developed on the hot-wire. They proposed a model in which an oil coating build up on the hot-wire due to oil deposition up to some point, then broke off. This process would continually repeat itself. Falco and Abell did note the size of the coating appeared to be dependent upon resistance ratio. At a resistance ratio of 1.3, the oil accumulation upon the hot-wire caused a slow increase in the mean output voltage followed by a sudden return to normal. During this time the frequency response was found to decrease.

Measurements performed by Falco and Sniegowski also indicate that the oil fog has a large effect on hot-wire anemometers. Their data suggests that for resistance ratios less than 2.0 substantial errors could occur in velocity measurements. In addition, the oil fog caused large changes of the parameters m of the Collis and Williams relationship.

Since the results of previous investigations are somewhat contradictory the object of this study was the careful measurement of the changes in the heat-transfer characteristics of hot-wires operated a fog of mineral

oil droplets. All of the previous data was obtained at velocities of 15 m/s and higher. Due to constraints on the intensity of available light sources, typical flow visualization experiments currently operate at less than 6 m/s. This consideration resulted in all of the experiments in this investigation occurring in the range 1.9 m/s - 19 m/s. This then allows the data to be more helpful to researchers using these techniques. It also provides some overlap with the previous studies with oil fogs.

To verify that meaningful data can be obtained from a hot-wire operating in an oil fog contaminated atmosphere, it will be shown that the basic heat transfer relationship governing the hot-wire, the Collis and Williams relationship, is still valid. This will show that the hot-wire will not experience gross changes in its heat transfer characteristics.

CHAPTER 2
EQUIPMENT

2.1 Oil Fog Contaminants

The oil fog contaminants used in this investigation are generated from a white mineral oil marketed by Witco Chemical under the trade name of Blandol. This oil has a viscosity between 0.16 and 0.18 cm $^2/_s$ at 38°C. Boiling occurs at approximately 290°C.

The apparatus used to generate the fog was a C. F. Taylor 3020 smoke generator. This device created the oil fog or "smoke" by forcing mineral oil through capillary tubes where sufficient heat was supplied to vaporize the oil. The vaporized oil was then passed through a nozzle to condense the vapor into droplets. The droplets were then mixed with air to create the oil fog and introduced into the wind tunnel at a slight overpressure through a pipe network. According to literature supplied by the manufacturer, the diameter of the oil droplets produced by this device varied between 0.5 μm and 5.0 μm.

2.2 Hot-Wire Characteristics

The hot-wires used for this experiment were constructed from tungsten wire. The wire had a diameter of 5 micrometers and a sensing length of 1 millimeter, giving a length to diameter ratio for this wire of 200.

On both sides of the sensing region a copper coating was plated onto the wire. This allowed the wire to be soldered onto the probe supports. The wire supports were composed of 2 jeweler's broaches held in alignment by an epoxy body. This was then mounted on a brass sting. (See Figure 2.1).

In this investigation two hot-wire operating geometries were employed. The first geometry consisted of the hot-wire being operated normal to the flow direction, designated a straight or u-wire probe. In the second geometry employed, called the slant wire probe, the hot-wire was operated at a 45° angle to the oncoming velocity vector. These two configurations are shown in Figure 2.2. Additional configurations were not deemed necessary since these two geometries are the basic building blocks for all other configurations normally used in practice. The hot-wires were used in conjunction with Disa 55 M01 constant temperature anemometers.

The sensitivity of the wire, the ability of the wire to differentiate small changes in velocity is governed by the difference between the wire temperature and the ambient fluid temperature. The parameter which governs the hot-wire operating temperature is the ratio of resistance a wire has at the operating temperature to the resistance of the wire at the ambient air temperature. This ratio is termed the hot-wire resistance (R) or overheat ratio. From this ratio the operating temperature of the hot-wire can be determined using the relationship

$$T_O = T_A + \frac{1}{.004}[R-1], \text{ in } {}^{0}C$$

The resistance ratios that are normally used in practice with hot-wire probes constructed of tungsten fall between R = 1.8 and R = 1.3. In this investigation, three resistance ratios were investigated. These are 1.8, 1.6, and 1.45 which correspond to temperatures of 224°C, 174°C, and 150°C.

When the hot-wires were initially used, a slight amount of oxidation would take place. This oxidation increased the resistance of the hot-wires, thereby causing the output voltage to drift and subsequently yielding errors in measurement. To prevent this from effecting the results obtained, the hot-wires were operated at a resistance ratio of 1.8 for a period of 24 hours to allow them to stabilize. Operation at higher

resistance ratio caused severe oxidation of the tungsten to occur, often resulting in the destruction of the wire.

Many investigators use platinum wire as the sensing element of the hot-wire. This allows the hot-wire to be operated at a much higher resistance ratio without causing the destruction of the sensor. This material was not used for these experiments due to the possibility of the mineral oil and the platinum reacting chemically.

2.3 Wind Tunnels

The majority of the experiments performed in this investigation utilized a wind tunnel especially designed for the study. The wind tunnel is a vertical type. It is a 2-dimensional design with a 1.2 m long test section that is 15.25 cm high and 30.5 cm wide. The experiments performed in this wind tunnel required only the first 15 cm of the working section and were performed along the centerline of the wind tunnel. To insure a steady air flow into the working section, a 9.71 area ratio contraction was used in conjunction with screens and a honeycomb. A fan of sufficient size was employed to allow the flow velocity to be varied from 0.15 m/s to 22 m/s.

Figure 2.3 shows this wind tunnel. Also shown is the pipe network used to introduce the oil fog in the flow field. This network consisted of copper pipe of 1.27 cm inside diameter with a 90° elbow that brought the oil fog from the outside of the wind tunnel to the center of the contraction. Over this elbow was placed a 2.54 cm inside diameter pipe 60 cm long. It was suspended by a 0.976 cm rod running through it 11.4 cm from its upper end. This allowed further carburizing of the oil fog. The upper end of the large pipe ended 5 cm inside of the wind tunnel test section. The hot-wires to be tested were positioned 0.63 cm over the pipe outlet, directly in its center line. The pipe provided the benefits of containing the oil fog over a precise area and also providing a visually uniform oil fog distribution over the hot-wire for all the flow velocities used. This arrangement, with the wind tunnel exhausting into the atmosphere, allowed

the hot-wire to be subjected to a constant oil fog concentration for long periods of time.

The experiments performed in boundary layers required a different wind tunnel. This wind tunnel, shown in Figure 2.4, was specially constructed for continuous flow visualization studies using an oil fog (see Falco 1980). The maximum velocity attainable in this facility is 6.4 m/s with an associated free stream turbulence level of 0.3 percent of the mean free stream velocity. The experiments were performed on a flat plate at a distance of 5.8 m from the leading edge.

CHAPTER 3
PROCEDURES

3.1.1 Measurement of Relative Oil Fog Concentration

The relative oil fog concentration in the neighborhood of the hot-wire was monitored using an optical technique. A coherent beam of light, supplied by a laser, was directed through the air stream immediately below the hot-wire sensing element. The opacity of the oil fog was then measured using the apparatus shown in Figure 3.1.

The primary components of the apparatus included a 1mW Helium-Neon laser, two photodiodes with their associated signal amplifying circuits, a voltmeter to monitor the photodiode output voltages, and a beam splitter. The two photodiodes and their circuits were identical. One photodiode unit was used to measure oil fog concentration while the other was used to monitor the variations in the output of the laser. The beam splitter was used to direct one-half of the laser emission to each of the photodiodes.

The photodiode and its circuitry were housed in the enclosure shown in Figure 3.1. The circuitry is shown in Figure 3.2, and is diagrammed in Figure 3.3. The photodetector used was a Hewlett-Packard model 4220 pin photodiode. The important properties of this device are shown in Table 3.1. Both the photodiode and its amplifying electronics exhibited a linear voltage response. The only adjustable parameter in this system was a d-c offset which allowed the output voltage to be nulled when there was no radiant larger radiation input to the photodiode.

The Spectra-Physics laser used in this apparatus emitted radiation at a frequency of 633 nm. The nominal output of 1mW was found to vary approximately $\pm$5%.

3.1.2 Calculation Of Relative Oil Droplet Concentration

The attenuation of a coherent beam of light by a fog of oil particles is governed by the equation

$$\frac{I}{I_0} = \exp\{-aL\}$$

also known as the Beer-Lambert Law. In this relationship I/I_o is the fraction of light transmitted, a is the extinction coefficient of a unit volume of aerosol, and L is the optical path length through the aerosol. Skinner and Boas-Traube (1947) have suggested that the extinction coefficient per unit volume can be expressed as

$$a = A_{EX}\, M_C$$

where A_{EX} is the droplet specific projected extinction area and M_C is the droplet mass concentration. By inserting this equation into the Beer-Lambert Law and solving for M_C, the expression

$$M_C = -\frac{1}{A_{EX} L} \ln (I/I_o)$$

is obtained which would allow the calculation of the droplet mass concentration in the neighborhood of the hot-wire is A_{EX} where known. The fraction of light transmitted is merely the ratio of the photodiode sensor output when oil fog is presented in the flow to the output obtained in clean air. This is a result of the linearity of the photodiode sensor response. Because A_{EX} was unknown, the above expression was used as a

basis for the definition of a relative, nondimensional oil fog concentration C, defined as

$$C = \ell n\ (I/I_o)$$

3.2 Mean Flow Velocity Calibrations

Measurements were made to calibrate hot-wire anemometer output voltages to the corresponding air velocity. The calibrations were in the Collis and Williams format of E^2 versus V^m, where E is hot-wire voltage and V is air velocity in m/s. The hot-wire calibrations were performed in clean air and three relative oil fog concentrations (0.18, 0.32, 0.47). Each calibration was obtained by maintaining the hot-wire resistance ratio and oil fog concentration constant while varying the air velocity. The air velocity was changed incrementally from 1.8 to 19.0 meters per second.

Because the flow field the hot-wires were calibrated in was turbulent, time averages were necessary. The reference air velocity was derived by measuring the static pressure in the neighborhood of the hot-wire and employing Bernoulli's equation.

For increased accuracy a computer controlled data acquisition system was used to obtain the calibration points. This system allowed the averaging of a sufficiently large number of hot-wire voltage values to obtain a statistically stationary mean hot-wire voltage value (175,000).

The data acquisition system consisted of a TI960A mini-computer that sampled voltage from a Disa 55M01 hot-wire anemometer and a Decker 308-3 pressure transducer. The analogue voltage outputs from the hot-wire anemometer and the pressure transducer were converted to digital form by a 10 bit analogue-to-digital converter. The hot-wire anemometer signals

were first analogue filtered at 20 kilohertz before they were digitized at a rate of 1.75 kilohertz.

An assembly language computer code named CALTAP controlled the data acquisition. Once the program obtained the required number of data points, the average of both the hot-wire anemometer and the pressure transducer voltages would be calculated. The program would then convert the mean pressure transducer voltage to a static pressure (in inches of water) using a second order polynomial calibration equation. The mean pressure value, h, was then converted to the mean velocity by the equation

$$V = 15.89 \sqrt{\frac{T}{b}} \sqrt{h}$$

where

T = ambient temperature

b = ambient pressure

The hot-wire voltages and corresponding air velocities for each calibration were subsequently fitted to the Collis and Williams relationship on an IBM 1800 computer using a Fortran program named CALFT (see Appendix). The program outputted the values of the parameter E_o^2, k, and m of the Collis and Williams relationship that provide the best fit to the data. Also calculated by this program were values of the hot-wire sensitivities, dV/dE, and the standard deviation of the calibration data.

The manner in which CALFT calculates the values of E_o^2, k and m is via a non-linear estimation. The value of m is initially assumed to be 0.45. A linear regression analysis is then performed on the hot-wire voltage and velocity points to compute values of E_o^2 and k. The hot-wire voltage data points are then converted to velocities using the calculated parameters. The standard deviation of the calculated velocity values and the measured

values is then determined. A new value of m is then chosen and the processes is repeated until the standard deviation of the calculated velocity values to the measured ones is minimized.

To allow additional insight to be obtained into the effects of the oil fog on the hot-wire, the parameters E_o^2 and k were calculated assuming m fixed at a value of 0.45. This was performed by performing a linear regression upon the data points obtained by the CALTAP code. The analysis was performed with a Hewlett-Packard HP-55 calculator. In addition, an estimate was obtained of the accuracy with which the data points could be reproduced with the calculated linear relationship. This estimate, designated F, was determined using the equation

$$F^2 = \frac{\left[\sum(E^2-\overline{E^2})\,(V^{\cdot 45}-\overline{V^{\cdot 45}})\right]^2}{\sum(E^2-\overline{E^2})^2\left[\sum(V^{\cdot 45}-\overline{V^{\cdot 45}})^2\right]}$$

A value of 1 indicates a perfect fit to the data points.

The data acquisition system and the two programs CALTAP and CALFT were developed by Dr. J. F. Foss of Michigan State University.

3.3.1 Measurements of Fluctuating Quantities

These measurements were obtained in the same wind tunnel as the mean flow measurements. As before the hot-wires (u and slant) were operated at a selected resistance ratio and air velocity. The oil fog concentration in the neighborhood of the hot-wire was then set to the desired value. The hot-wire was then operated under this "steady state" condition and the measurement made. The experiment was then repeated until the entire range of oil fog concentrations (from clean air to a relative oil fog concentration of 0.47) had been traversed. The air velocity was then incremented and the above procedure repeated. Upon completing the measurements for

the various velocities, the wire resistance ratio would be altered (from 1.45 to 1.8). This procedure was employed for both types of hot-wires.

A Thermo Systems Inc model 1076 rms voltmeter was used to measure the rms voltage of the unfiltered hot-wire anemometer signal. The rms voltage output from this device was then averaged for a period of 7 minutes by a Disa 52B20 integrator to obtain a stable value. For each permutation of the parameters, from 4 to 6 experiments were performed and the results averaged.

The rms voltage values from the hot-wire and the voltage from the photo-diode detecting the oil fog opacity were input minually into a VAX computer. The program RMSREDU (see Appendix) was then used to calculate the relative oil fog concentration for each data point. The experiments comprising each permutation were then averaged together to obtain a mean hot-wire resonse curve to oil fog concentration. Hot-wire rms voltage value were calculated for incremental oil fog concentration values by linearly interpolating between the data points from each experiment. These value were then averaged for like permutations of the hot-wire parameters to obtain the rms voltage response curves.

3.3.2 Hot-Wire Anemometer Spectral Response

Energy spectra for hot-wires operated in both clean air and a relative oil fog concentration of 0.32 were obtained at two velocities. To obtain the amount of flow energy at various frequencies, a Hewlett-Packard wave analyzer was used. The wave analyzer acts as a precise narrow band pass filter operating in the frequency domain. With the hot-wire resistance ratio, air velocity and oil fog concentration held constant during an experiment, the rms voltage was measured at predetermined frequencies between 100 Hz and 20 Khz. The rms voltage passed by the wave analyzer at a given frequency was measured with the TSI model 1076 rms voltmeter. The voltage output from the voltmeter was then averaged by the Disa 52B20 integrator for a period of 7 minutes.

When this experiment was completed, the oil fog concentration was in the neighborhood of the hot-wire was varied and the experiment was repeated. Next, the air velocity was changed and the process repeated again.

To obtain the spectral data a Hewlett Packard wave analyzer was inserted into the above chain of instruments after the anemometers and before the rms voltmeters.

3.4 Instantaneous Measurements

The photographs of the boundary layers with the oscilloscope tracings of hot-wire and photomultiplier signals were supplied by Dr. R. E. Falco. These were obtained using special facilities. A flow visualization wind tunnel was used that allowed the introduction of the oil fog into a laminar boundary layer. The boundary layer was then tripped to cause it to become turbulent. A hot-wire of the U type was installed in the wind tunnel a large enough distance from the wall to allow the hot-wire to come into contact with the oil fog filled regions of the boundary layer and clean air regions of the free stream for an approximately equal amount of time. The photomultiplier tube was then focused immediately underneath the hot-wire. A 5 watt argon-ion laser was then used to illuminate a 2 millimeter thick vertical slice of the boundary layer in the same plane as a probe. Light from the laser was spread into a sheet by allowing the beam to strike a cylindrical lens. When the probe entered an oil fog containing region, laser light scattering off the oil fog particles was detected by the photomultiplier tube. The signals from the hot-wire anemometer and the photomultiplier tube were then displayed on the oscilloscope. Through the use of mirrors the image of the oscilloscope screen was then photographed with the boundary layer. These photographs resulted in 20 events of the hot-wire entering a oil fog contaminated region. The hot-wire signals were then digitized and normalized in time and voltage and ensemble averaged.

3.5 Boundary Layer Experiments

Two experiments were performed in fully turbulent boundary layers. The first consisted of measuring a turbulent intensity distribution in a boundary layer. For this experiment a hot-wire was traversed through a boundary layer. Measurements were taken at preselected heights from the wall. Turbulence intensities were intially measured in clean air and then in oil fog contaminated air using the same hot-wire probe. For these measurements a TSI 1076 true rms voltmeter was used to obtain the rms voltage of the signal. The rms voltage signal was then averaged for a period of 7 minutes by a Disa Electronics 52B20 Integrator.

The second boundary layer experiment consisted of digitizing hot-wire voltage records of a hot-wire operated in clean air and a hot-wire operated in oil fog contaminated air. A 10 bit analog to digital converter was used for this purpose in conjunction with Disa 55M01 constant temperature anemometers. The output voltages from the anemometers were high passed filtered at 20 kilohertz to remove noise and then digitized at a rate of 1.75 kilohertz. All of the velocity records contain 1,050 data points.

CHAPTER 4
RESULTS

4.1 Mean Flow Calibration

Figures 4.1 - 4.5 demonstrate the effect oil fogs of various mass concentrations have upon the voltage-velocity calibration curves of hot-wire anemometers. Quantitatively using the clean air data as a baseline, the data exhibited four trends:

(1) The change in the calibration increased as the oil fog concentration was increased;

(2) The change in the calibration, for a given oil for concentration, decreased with increasing probe temperature;

(3) The slant wire demonstrated less sensitivity to the oil fog than did the straight wire;

(4) The standard deviation of the data points increased with increasing oil fog concentration.

The manner in which the numerical values of the Collis and Williams parameters E_o^2 and k are altered by the oil fog is tabulated in Tables 4.1 (m is constant) and 4.2 (m is allowed to vary). The oil fog has the greatest effect upon the parameter k (Table 4.1).

4.2 Hot-wire Sensitivity

An examination of hot-wire sensitivity values (Table 4.3) yields additional insight. Straight wires experienced an increase in the sensitivity as the oil fog concentration was increased. The percent increase was greatest at the lowest velocities and decreased as the

velocity was increased. The operation of straight wires at lower temperatures resulted in greater relative increases in the sensitivity for a given oil fog concentration.

Slant wires demonstrated a much more complex behavior. The change in the sensitivity for the slant wires tended to be less than for straight wires given similar conditions. In addition, the slant wire's sensitivity at the highest oil fog concentration tested was at all times less than the wire's sensitivity in clear air.

4.3.1 RMS Voltage Measurements

Figures 4.6 - 4.9 show the effect oil fog has upon the rms voltage measured by a hot-wire. The measurements show that the oil foy introduces only very small errors into the rms measurement. For both types of hot-wire geometries, the largest error measured for a hot-wire operated at a resistance ratio of 1.8 was 4.5%.

The rms voltage measured in the oil fog contaminated air was dependent upon the oil fog concentration. The degree to which the oil fog effected the measurement was strongly dependent upon the operating temperature of the sensor. The oil had increasing effect upon the hot-wire measurement accuracy as the sensor temperature was decreased.

A behavior was observed for all instances except for the lowest speed slant wire results. At low oil fog concentrations the measured rms voltage was less than the clean air value. As the oil fog concentration increased, so would the measured rms voltraged. A second interesting phenomena evidenced was as the velocity was increased from 1.9 m/s to 4.5 m/s the rms voltage measured would decrease. As the velocity was increased further, to 9 m/s, the rms voltage value increased to a value larger than the 1.9 m/s value.

Figure 4.10 compares straight and slant wire rms voltage response as a function of oil fog concentration. The resistance ratio is constant at 1.8. At each of the three velocities, the straight and the slant wire results are very close in form. They differ only in that the slant wire curves generally fall above the straight wire curve.

Figures 4.11 and 4.12 show oscillograms of the hot-wire signal as a function of velocity and concentration. For both figures the straight-wire was operated at a resistance ratio of 1.8. Figure 4.11 demonstrates the effect increasing the oil fog concentration has upon a hot-wire operated at 1.9 m/s. The oil fog causes large, positive voltage spikes that increase with concentration. The increased temporal resolution oscillograms show that the spikes consist of a sudden voltage increase, indicating a sudden cooling of the hot-wire, followed by an exponential type decay to the apparent mean voltage. The time duration of the spikes are typically .01 msec or less and they have amplitudes ranging up to .1 Volts.

Figure 4.12 shows that a similar situation occurs at the higher velocity, 9.4 m/s. At the higher velocity, the spikes are much less evident and appear only to occur at high relative oil fog concentrations, 0.53. At this flow velocity, it is difficult to distinguish the spikes from the turbulent fluctuations.

4.3.2 Energy Spectra

The energy spectra obtained in clean air and at a concentration are shown for the two velocities in Figures 4-13 and 4-14. At low velocities, the effect of the spikes is clearly visible between the frequencies of 1200 hertz to 10 kilohertz. The lower frequencies show a higher energy due to the oil fog. This may be due to aliasing of the oil fog spike signals. However, due to difficulties in interpreting energy spectra care must be used when drawing conclusions from this result. At higher velocity the effect of the spikes at higher frequencies is not visible in the data. At the lower frequencies the higher power due to the oil is again present.

4.4 Instantaneous Data Measurements

During the acquisition of the rms data, hot-wire signal fluctuations similar to those observed by Falco and Abell were observed. When the hot-wire was operated at resistance ratios of 1.45 and relative oil fog concentrations above 0.32 very large low frequency voltage fluctuations were observed. The mean voltage could be observed to slowly increase in value well above the magnitude of the largest turbulence fluctuation. This increase would occur slowly over a period of approximately 1 minute. The amount of time required was dependent upon the oil fog concentration. The voltage would then suddenly return to normal in a very short time, considerably less than a second. During the time this phenomena was occurring to the mean hot-wire voltage, the rms voltage was also affected. The rms level would slowly decrease during the period of time that the mean voltage was increasing. At the time the mean voltage achieved its maximum, the rms voltage was very near zero. The rms voltage would then return very quickly to normal at the identical time that the mean voltage returned to normal.

Figure 4-15 is a typical photograph used to examine the impact of a transient oil fog concentration. The photograph shows a hot-wire being operated in the intermittent region of a oil fog contaminated boundary layer. The two traces are those of the hot-wire anemometer output and the photomultiplier output. The photomultiplier was used to indicate whether the hot-wire was in a oil fog contaminated region. 20 such events were ensemble averaged to yield Figure 4-16. The 20 digitized events were ensemble averaged two ways. First all 20 were averaged. Second the signal that had a voltage increase upon entering a oil fog contaminated region were averaged separately from those that had a voltage decrease upon entering a oil fog contaminated region. Of the 20 signals, 12 increased upon entering a oil fog contaminated region.

From Figure 4-16 it can be seen that there is no appreciable bias of the hot-wire signal introduced when the hot-wire strikes the oil fog boundary. Once inside the oil fog contaminated region the velocity begins to drop as it should in the boundary layer. There is no sharp discontinuity in the voltage signal brought about by the hot-wire contacting the oil fog contaminated region. When the hot-wires exit the oil fog contaminated regions the signals once again vary very smoothly across the boundary, showing no sign of discontinuity.

4.5 Boundary Layer Measurements

Because the data presented suggests that a hot-wire operated at a resistance ratio of 1.8 may not require special calibration when used in an oil fog, the turbulence intensities in a boundary layer were measured in clean air and an oil fog concentration of the measurements were performed on a flow with a free stream velocity of 3.2 m/s which resulted in a Reynold's number based on the momentum thickness of 2,700. The reduced data is shown in Figures 4-17 and 4-18. Figure 4-17 shows the data obtained in the outer part of the turbulent boundary layer being compared to data obtained by Klebanoff (1954) and Blackwelder and Kovasznay (1970) in turbulent boundary layers. The clean air values and the data obtained in the oil fog agree quite well throughout the boundary layer. The data also agrees quite well with the data obtained in the wall region of a turbulent boundary layer. The data obtained by Klebanoff and Ueda and Hinze (1975) is also plotted for comparison. The data obtained in clean and in oil fog contaminated air show very good agreement. The difference in the values is much less than the scatter that occurs from one experimenter to another. These measurements do indicate that the largest difference between clean air and oil fog measurements occur when the turbulence intensities are highest.

The effect the oil fog has on data obtained digitally is shown in Figure 4-19. This figure shows four hot-wire voltage records of 1,050 points each. A sampling rate was fixed at 1.75 kilohertz and the flow velocity is approximately 2 m/s. Records a were obtained in clean air

while records b were obtained in oil fog comtaminated air at a relative concentration of 0.32. The difference in the signals is the presence of the very high voltage spikes in voltage signals of the hot-wires operated in the oil fog. These spikes were composed of a single point on the data records. The spikes are due to the same phenomenon shown in the oscillograms in Figure 4-11. Of the data records examined for spikes, most contained one or no spikes.

CHAPTER 5
DISCUSSION

5.1 Operational Considerations

The results obtained in this series of experiments show that accurate hot-wire measurements can be made in an oil fog. When making hot-wire measurements in this type of environment the hot-wire should be operated at a resistance ratio of 1.8 and at the lowest oil fog concentration possible.

If a hot-wire is operated at a resistance ratio of 1.8 and a relative oil fog concentration of less than 0.47 errors of less than 3% can be expected in average velocity measurements for a hot-wire calibrated in clean air. If additional measurement accuracy is required , the hot-wire should be calibrated in a flow containing the oil fog concentration expected. In addition, if the flow velocity is kept below 5 m/s, errors in the average rms voltages measured are negligable. This allows accurate intensity measurements to be made in an oil fog with a hot-wire calibrated in clean air.

The oil fog can cause difficulties during the calculation of higher order statistics, correlations and energy spectra when unfiltered or improperly filtered hot-wire signals are used. These difficulties are due to the high frequency spikes on the hot-wire signals caused by the oil fog.

To obtain accurate data, care must be taken to ensure that the signal frequency of the oil fog spikes is not contained within the frequency range of the turbulence. If the spikes are outside the range of the turbulence the signal can be low pass filtered to remove the oil fog spikes. For some applications, the oil fog spikes in the unfiltered signals may significantly contribute to the variance of the velocity measurements. The skewness of the fluctuations will be biased because the oil fog spikes are always positive. Finally, the kurtosis of measurements made in an oil fog will be increased because the oil fog spikes are a high

frequency phenomena. The resolution of energy spectra will be reduced because the oil spikes appear as an additional noise source.

All of these effects can be removed for low speeds (5 m/s) by digitally filtering the hot-wire signal. The digitized signals shown in Figure 4.19 show that due to the high frequency nature of the oil fog spikes (2kHz), the oil fog spike is only identified by a single digital data point. In addition, the frequency content of the turbulence is below the frequency of the oil fog spikes. The effect of the spikes can be removed by either frequency filtering or locally smoothening the hot-wire signal.

5.2 Physical Model

The changes in hot-wire calibrations demonstrate that oil fog has a definite effect. The increase in slope of the calibration curves is a result of an increase in the transfer of energy from the hot-wire to the air. To assist in the interpretation of the cause of this the hot-wire sensitivity results must be examined. The difference in a hot-wire's sensitivity when operated in oil fog as compared with clean air is similar to the sensitivity difference resulting from the comparison of hot-wires of differing diameters. This effect is documented in data obtained by Richardson and McQuivey (1968), Figure 5.1. Here it can be seen that as the diameter of the sensor is increased the sensitivity increases. By comparison the oil fog must be creating a coating on the hot-wire. A thin coating of oil would both increase the heat transfer and increase the apparent sensitivity of hot-wire. Similar conclusions can be reached from heat transfer considerations. The rate of heat transfer from a hot-wire with or without an oil coating will be controlled by the convection process. If the assumption is made that there is an oil coating upon the wire, conduction of heat will occur from the wire to the mineral oil, at a much higher rate than the convection process. A heat balance between this conduction and

convection from the outer surface of the oil film to the air shows that the rate of heat flow through the hollow cylinder of oil

$$q = \frac{2\pi L(T_i - T_\infty)}{\frac{\ln(r_o/r_i)}{K} + \frac{1}{r_o h}}$$

is inversely proportional to the logarithm of the outer radius. Because the heat dissipation is directly proportional to the outer radius the heat transfer may be enhanced or retarded depending upon the thickness of the oil coating.

The thickness of the oil coating appears to be velocity related. At high velocities, a hot-wire's sensitivity characteristics (Table 4.3) are altered to a smaller degree than at low speeds. The coating thickness also appears very strongly dependent upon the sensor temperature. Apart from the initial oil build-up, the coat must remain relatively constant in size, maintaining a balance between oil evaporation, fluid dynamic drag attempting to remove the coating, flow along the sensor support needles and impinging oil droplets. This behavior is unlike dirt coatings. Dirt tends to accumulate on a hot-wire causing the heat transfer characteristics to constantly change. When operated in an oil fog at a given air velocity and oil concentration, hot-wire calibration remains constant over time.

The shape of the curves of the hot-wire rms voltage data could result from these competing effects. At low oil fog concentrations, the rms voltage signal is only slightly damped, if it is effected at all. At higher oil fog concentrations the rms voltage shows an increase over the clean air results. When this data is interpreted in light of the oscillograms showing large voltage spikes, definite conclusion can be drawn. At low oil fog concentrations the oil coating is decreasing the sensor's frequency response very slightly, more than the spikes contribute to the rms voltage because the number of spikes are few. As the oil fog

concentration increases, the number of spikes increases which causes an increase in the rms voltage. As the oil fog concentration becomes large enough the rms voltage increase due to the voltage spikes becomes larger than the decrease due to oil coating on the wire.

The oscillograms of the oil fog spikes reveal a substantial amount of information. The spikes are periods of enhanced heat transfer from the hot-wire. Goldschmidt and Householder (1969) showed that when small oil droplets of approximately 16 micrometers in diameter were dropped on a 5 μm hot-wire, a characteristic cooling signal resulted, Figure 5.2. Goldschmidt, et. al., concluded that the signals were due to the hot-wire heating the oil droplets to the hot-wire's operating temperature, where they evaporated. Since the voltage spikes obtained in this investigation have a very similar shape to those obtained by Goldschmidt and Householder, there is a prossibility they are due to the energy input required to heat the oil droplets impacted upon the hot-wire. Another hypothesis is that the spikes are a result of oil ripping off of the hot-wire. Which hypothesis is true cannot be determined from the available data. An additional mechanism, the evaporation of the oil, may affect the size of the oil coating on the wire, however, the importance of this mechanism is not known.

The oscillograms taken at 9.4 m/s reveal voltage spikes of smaller amplitude than those for the lower velocity case. The data indicates that less oil is being deposited upon the wire when an oil droplet impacts upon the hot-wire resulting in less oil remaining on the wire. Possible explanations for the lower amplitude spikes are:

1. Smaller oil droplets striking the hot-wire
2. Oil droplets shatter upon impact with the hot-wire
3. Smaller oil droplets ripping off the hot-wire

The first explanation, while possible, is unlikely as during the course of the experiments, no changes were made to the particle generation apparatus. Therefore, it is assumed the same particle size distribution

was generated throughout. The second explanation is much more plausible. Figure 5.3 reveals the maximum velocity with which an oil droplet can impact a solid object without shattering. Droplets of 5 μm diameter or larger cannot withstand an impact at a velocity of 10 m/s with a hot-wire without shattering. This would leave less oil on the hot-wire. The third explaination is equally plausible as the aerodynamic drag on the oil coating would be higher, reducing the steady-state size of the oil coating. This would imply that each oil droplet ripped off would be smaller in size than those ripped off at lower speeds.

Examination of the energy spectra shows a definite increase in energy throughout the frequency range measured. This occured at both high and low velocities. At low velocities the frequency range containing turbulent energy is below 1500 Hz. The higher frequencies show a substantial amount of noise. This was found by Morrow and Kline, Figure 5.4, to occur to hot-wires operated in water contaminated with dirt, demonstrating there is some similarity in the effect the two types of contaminants have upon the behavior of a hot-wire. At higher velocities the noise is not evident. This is consistent with the notion of a decrease in the amount of oil that remains attached to the hot-wire at higher speeds.

From the data obtained in this series of experiments, a model can be hypothesized to explain the physics of the phenomena occurring on and near the hot-wire. This model is similar to the one originally proposed by Falco and Abell. When a hot-wire anemometer is operated in an oil fog at temperatures less than the boiling point of the oil, a coating of oil develops around the wire. The thickness of coating is being maintained constant by the oil droplets striking the wire and simultaneously the oil composing the coating being torn off the wire by aerodynamic forces. The size of the oil coating is dependent upon these mechanisms and upon the surface tension of the oil, which is in turn dependent upon the wire temperature. At low velocities, the oil coating would be thicker than at high velocities due to the aerodynamic drag being small. Also at low velocities, an oil particle striking the wire would remain attached to the

wire due to the droplet having insufficient momentum to shatter as it strikes the hot-wire.

As the velocity is increased, the size of the oil coating decreases and the number of oil droplets striking the wire for a given interval would increase. At high velocity, the oil droplets shatter upon striking the wire leaving very little oil deposited on the wire per droplet impact. In addition, aerodynamic drag ripping off droplets would cause the oil coating to be very small even as a greater number of droplets impact the hot-wire.

Tilting the wire at a 45° angle to the oncoming flow complicates the above affect further and may allow additional, unknown forces to occur. At a resistance ratio of 1.8, the oil fog has no affect on the hot-wire response at low concentrations. As the concentration is increased, the hot-wire begins to show the same trends as the U-wire. Figure 4.10 shows that above a concentration of the curve for the U-wire and the slant-wire are very much identical with the exception of the 2 percent upward shift of the slant wire data. The shift suggests that the oil build up on the slant-wire is not as large as on the U-wire.

CHAPTER 6
CONCLUSIONS

From the results obtained in this series of experiments, it has been found that an oil fog does not severely effect the response characteristic of hot-wires. It was also found that the Collis and Williams relationship held for hot-wires operated in an oil fog at all resistance ratios tested. When hot-wires were operated at resistance ratios of 1.8, the parameters in the Collis and Williams relationship were effected only very slightly at the oil fog concentrations typically used for flow visualization experiments (C=0.32). This shows that the heat transfer law for hot-wire anemometers is basically unaffected bythe oil fog, provided the hot-wire is operated at a sufficiently high temperature.

The oil fog tended to increase the rms voltage slightly. The increase was a function of the velocity, wire temperature, oil fog concentration and orientation of the wire. The error in an rms voltage measurement due to the oil fog was always less than 3% if the hot-wire was operated at a resistance ratio of 1.8 and the concentration was less than 1.1. Figure 6.1 depicts the range of the errors to be expected for a given oil fog concentration.

The energy spectra measured show errors of less than 12% in the frequency range that contains turbulent energy. At low air velocities, 2 m/s, the frequency ranges containing turbulence energy and noise are quite distinct. At higher air velocities, 9.5 m/s, the two ranges tend to merge into one another.

A model of the physics is presented based on the data obtained in this investigation. To confirm this model, I sugges that additional research be conducted on this topic. Basic points that must be examined are:

(1) What actually occurs when an oil droplet strikes the oil coated wire at various velocities. Experiments employing high speed photo microphotography would be very useful for this.

(2) What effects oil droplets of various diameters have upon a hot-wire's response.

(3) What occurs at approximately 4.5 m/s to cause the oil to have less effect on the rms voltage measured than at other velocities.

(4) How much is the rms voltage signal damped by the oil coating and increased by the voltage spikes and more importantly, is the basic signal modified to an appreciable degree.

The data just summarized in combination with the boundary layer measurements, show the excellent results that are attainable by calibrating a hot-wire in clean air at resistance ratio of 1.8, then using it in an oil fog contaminated air flow. A hot-wire can be operated in an oil fog at any resistance ratio above 1.45 providing a low oil fog concentration is used and the wire is calibrated in the oil fog.

APPENDIX

APPENDIX A

REFERENCES

1. Blackwelder, R. and Kovasznay, L. S.G., (1970), "Large Scale Motion of A Turbulent Boundary Layer With a Zero And a Favorable Pressure Gradient," Interm Tech. Report #2 To The U.S. Army Research Office, Durham, N.C.

2. Collis, D. C. and Williams, M. I., (1959) "Two-Dimensional Convection from Heated Wires at Low Reynolds Numbers," Journal of Fluid Mechics, Vol. 6 pp 357-384.

3. Falco and Abell, unpublished.

4. Falco, R. E., (1977) "Coherent Motions in the Outer Region of Turbulent Boundary Layers," Phy. Fluids, Vol. 20, pp. S124-S132.

5. Falco, R. E., (1980) "Combined Simultaneous Flow Visualization/Hot-Wire Anemometry for the Study of Turbulent Flows," J. Fluids Engr., Vol. 102, pp. 174-182.

6. Falco and Sniegowski, (1977) unpublished.

7. Fiedler, H. and Head, M. R. (1966) "Intermittency Measurements in the Turbulent Boundary Layer," J. Fluid Mech., Vol. 25, pp. 717-735.

8. Foss, J. F. (1967) "The Vorcom, Part II: Demonstration Vorticity Measurements," Third Annual Report NASA Langley Research Center.

9. Friehe, C. A. and Schwartz, H. W., (1968) "Deviations from the Cosine Law for Yawed Cylindrical Hot-Wire Sensors," Journal of Applied Mechanics, Trans. ASME, Vo.. 35, pp. 655-662.

10. Goldschmidt, V. W. and Householder, M. K., (1969) "The Hot-Wire Anemometer as an Aerosol Droplet Size Sampler," Atmospheric Environment, Pergamon Press, Vol. 3, pp. 643-651.

11. Hinze, J. O., Turbulence (1975), 2nd Edition, McGraw-Hill Book Company.

12. King, L. V., (1914) "On the Convection of Heat From Small Cylinders in a Stream of Fluid: Determination of the Convection Constants of Small Platinum Wires with Applications to Hot-Wire Anemometry," Philosophical Transactions, Royal Society, Series A, Vol. 214, pp. 373-432.

13. Klebanoff, P. S., (1954) "National Advisory Commission for Aeronautics Tech.," Note - TN 3178 (1954).

14. Morrow, T. B. and Kline, S. I., (1974) "The Performance of Hot-Wire and Hot-Film Anemometers Used in Water," Flow: Its Measurement and Control In Science and Industry, Vol. 1, pp. 555-562.

15. Richardson, E. V. and McQuivey, R. S. (1968) "Measurement of Turbulence in Water," Journal of the Hydraulics Division, ASCE, Vol. 54, No. HY2, Proc. Paper 5855, pp. 411-430.

16. Skinner, D. G. and Boas-Traube, S., (1947) "The Light Extinction Method of Particle Size Estimation," Inst. Chem. Engineers, Vol. 25, pp. 25.

17. Ueda, H. and Hinze, J. O., (1975) "Fine Structure Turbulence in the Wall Region of a Turbulent Boundary Layer," Journal of Fluid Mechanics, Vol. 67, pp. 125-143.

APPENDIX B

FIGURES

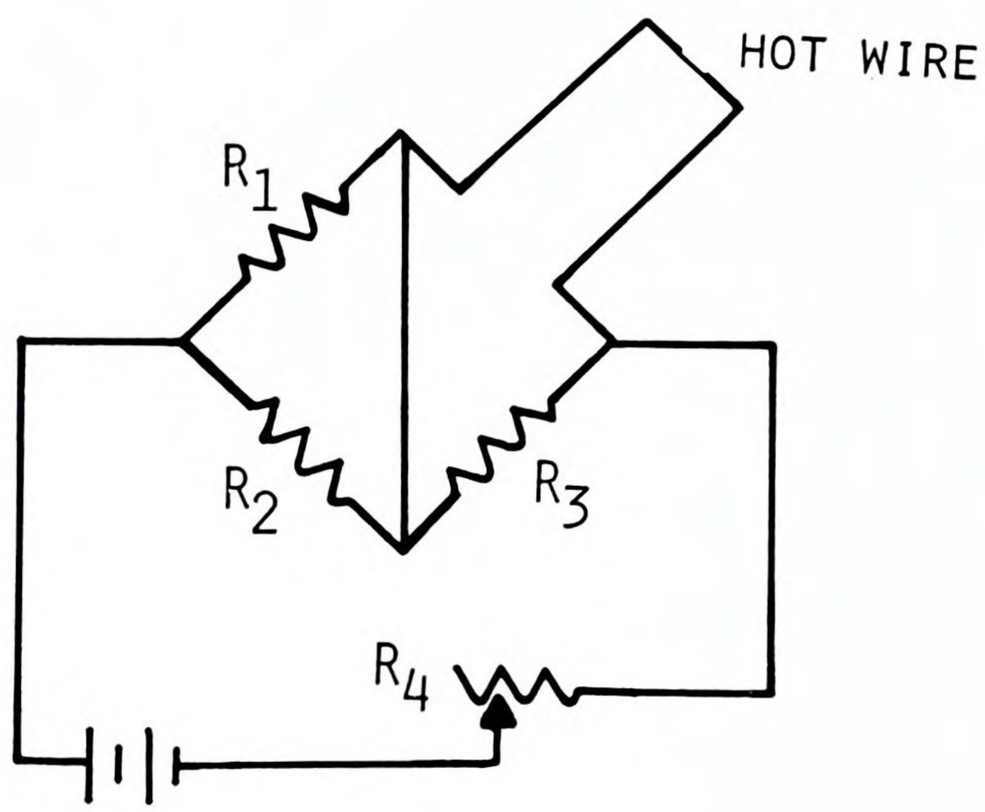

FIGURE 1.1 HOT-WIRE CIRCUIT DIAGRAM

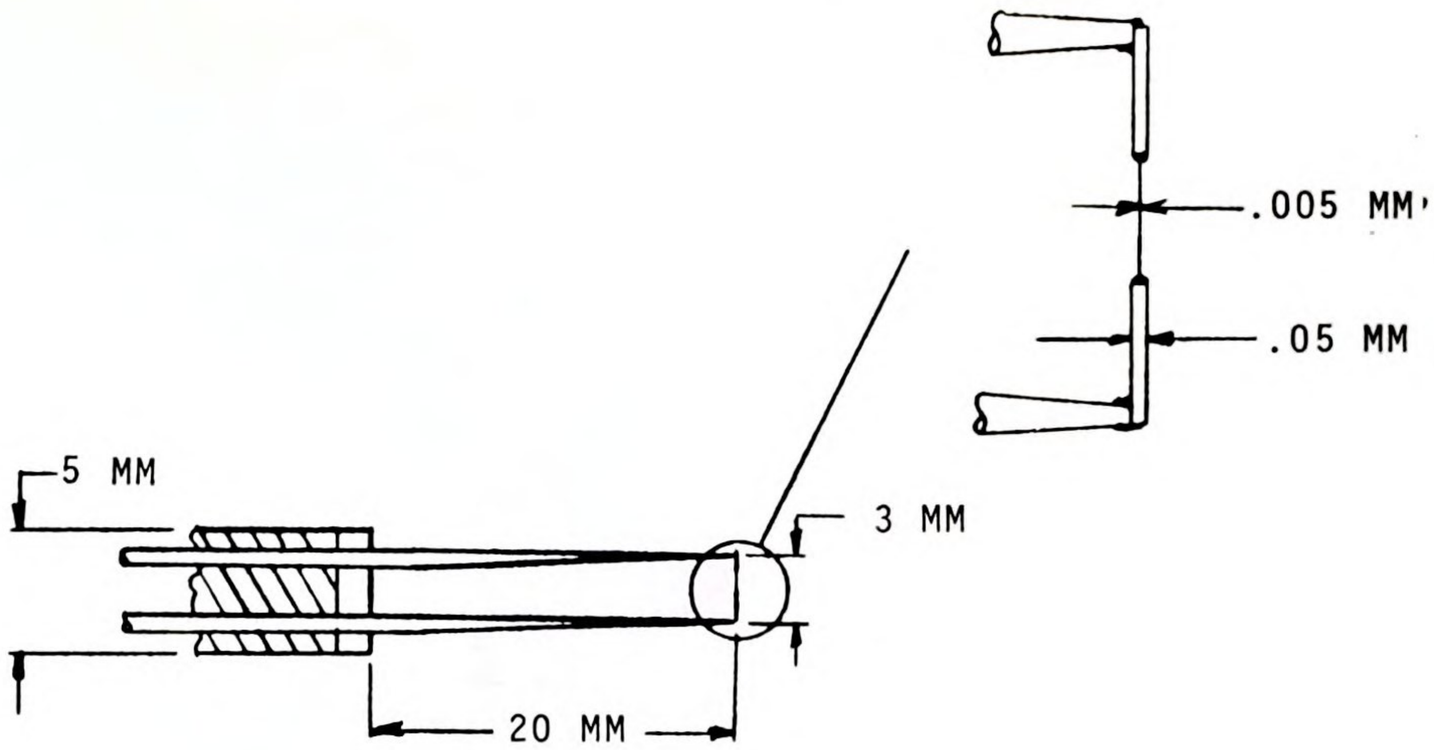

FIGURE 2.1 HOT WIRE PROBE

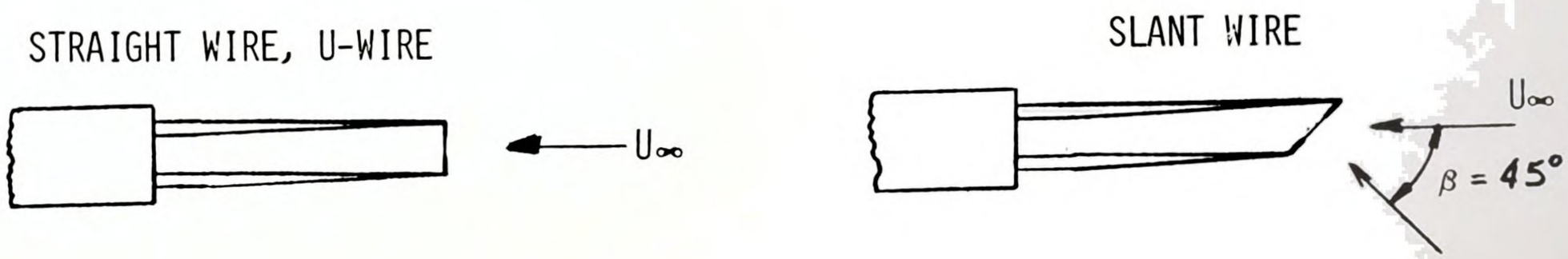

FIGURE 2.2 PROBE CONFIGURATION

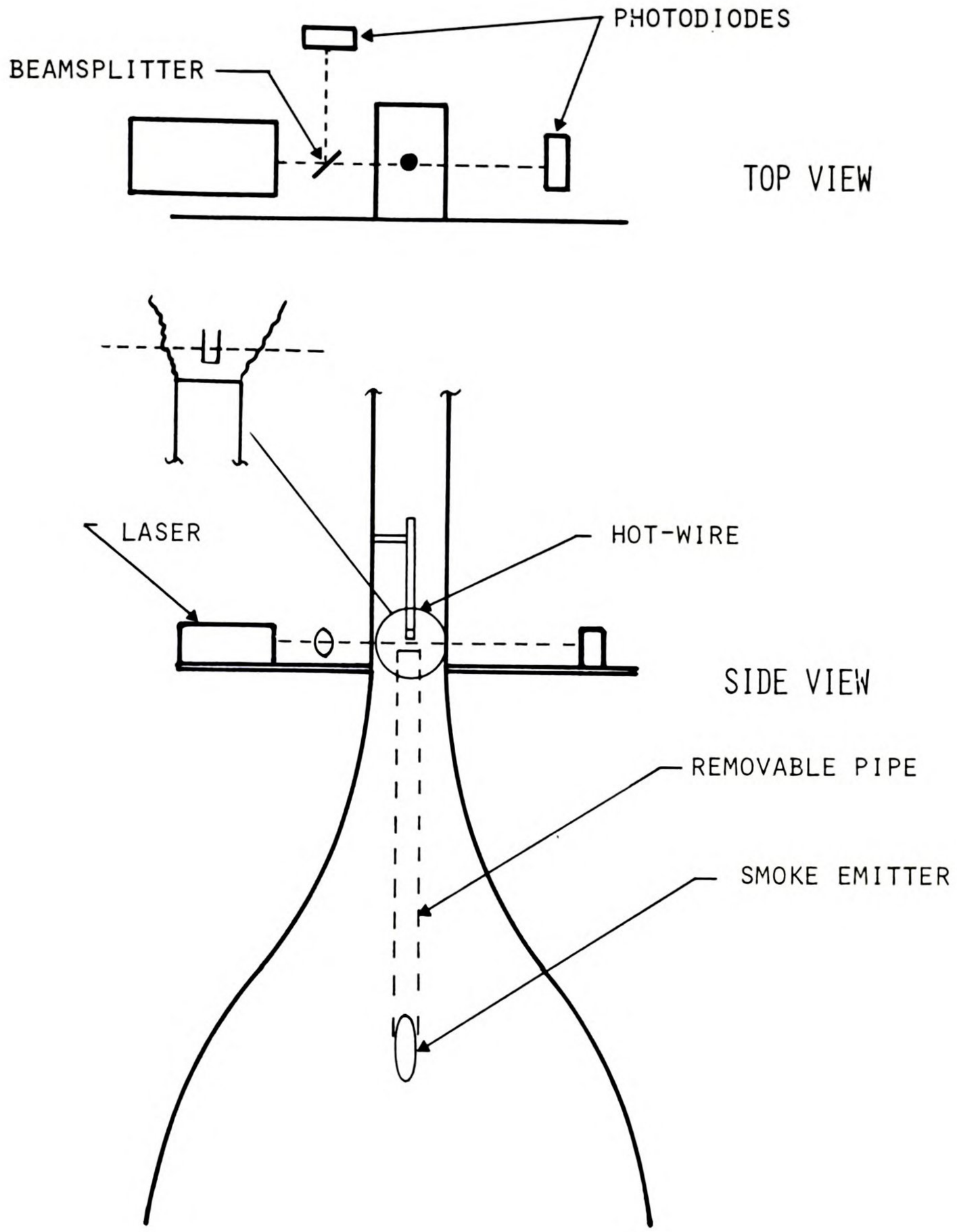

FIGURE 2.3 EXPERIMENTAL APPARATUS

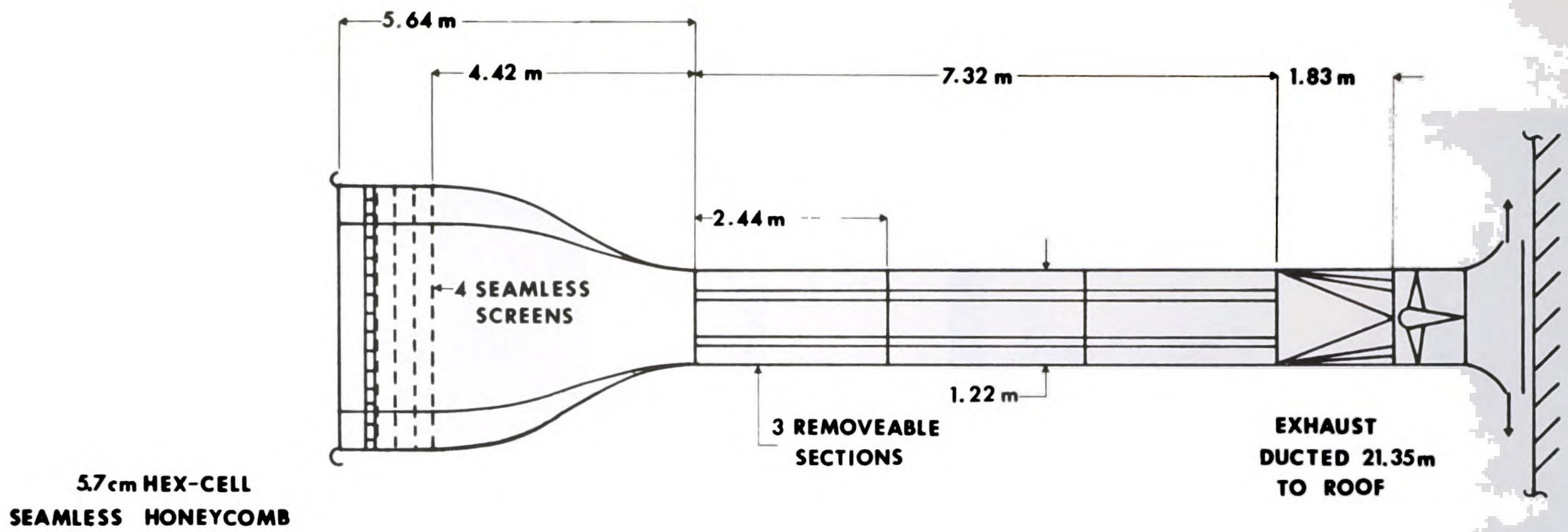

FIGURE 2.4 FLOW VISUALIZATION WIND TUNNEL

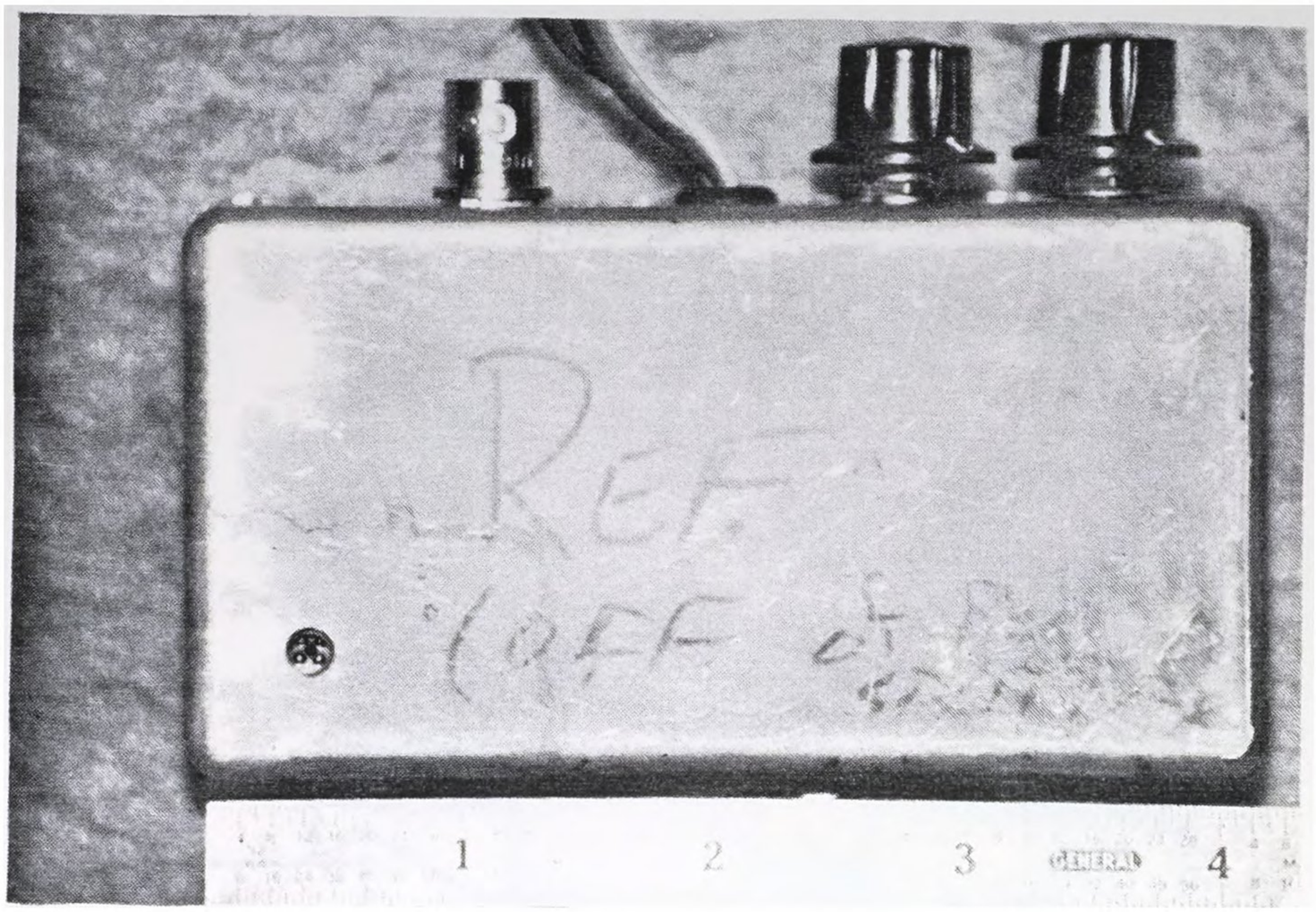

FIGURE 3.1 OIL FOG OPACITY DETECTOR

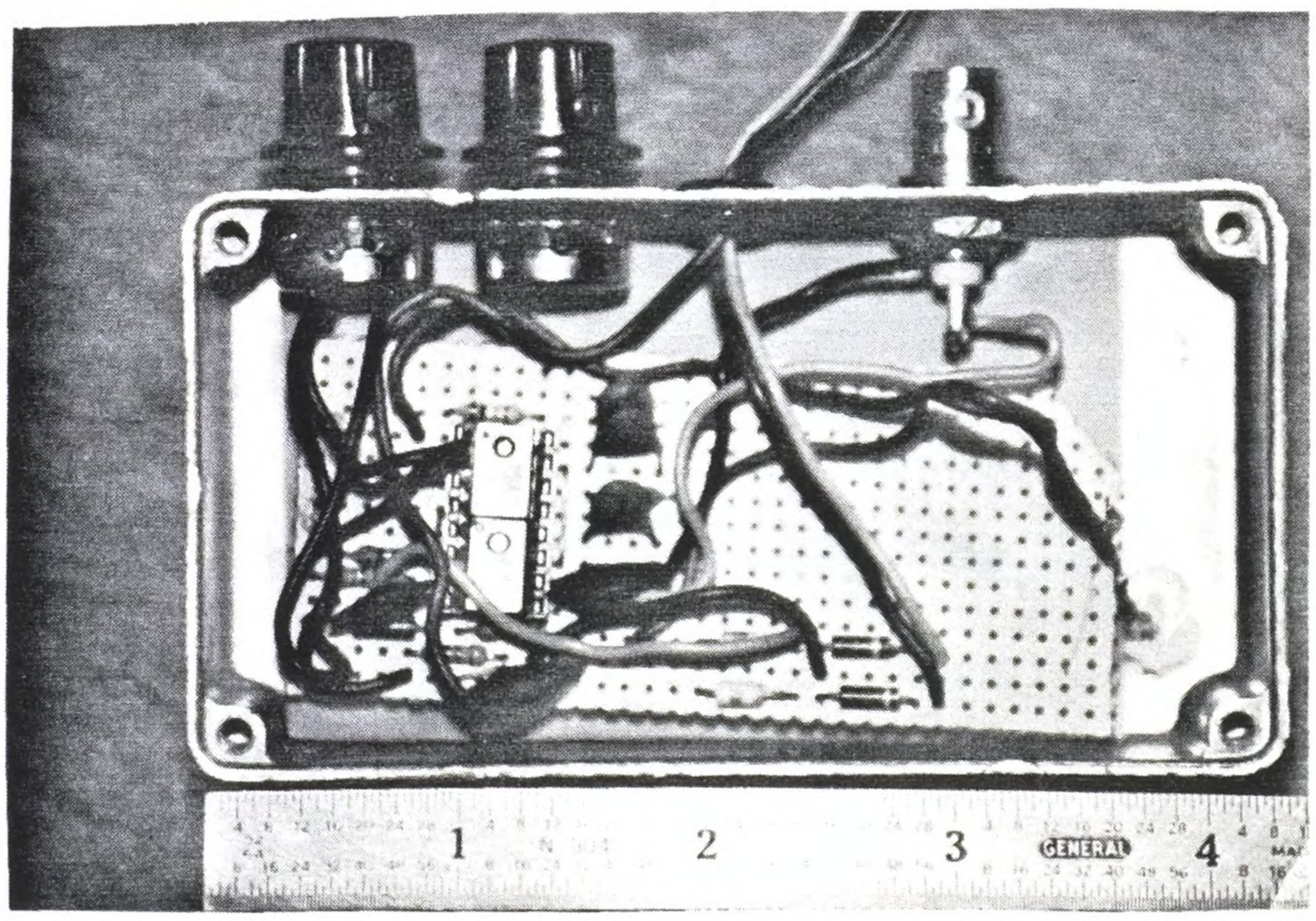

FIGURE 3.2 PHOTODETECTOR CIRCUITRY

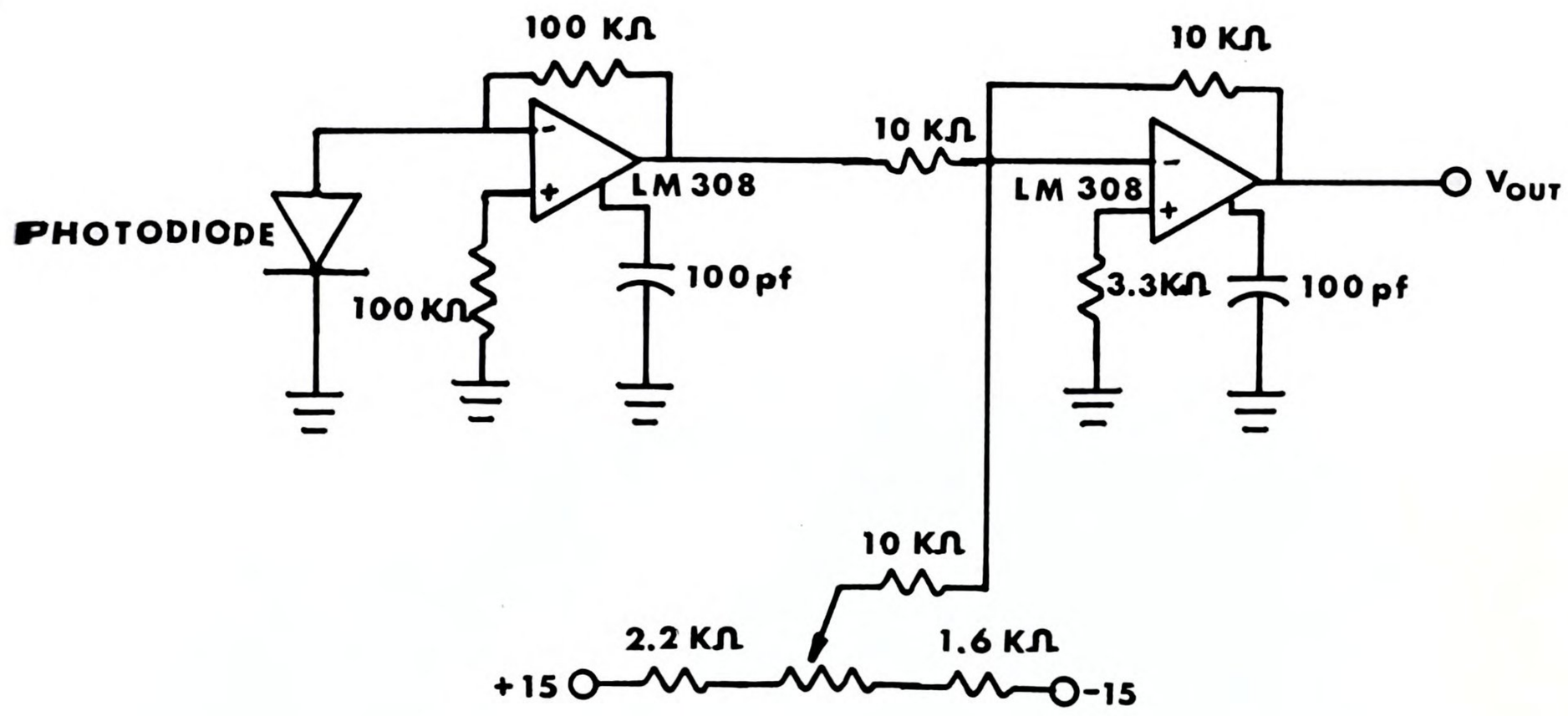

FIGURE 3.3 PHOTODETECTOR CIRCUITRY DIAGRAM

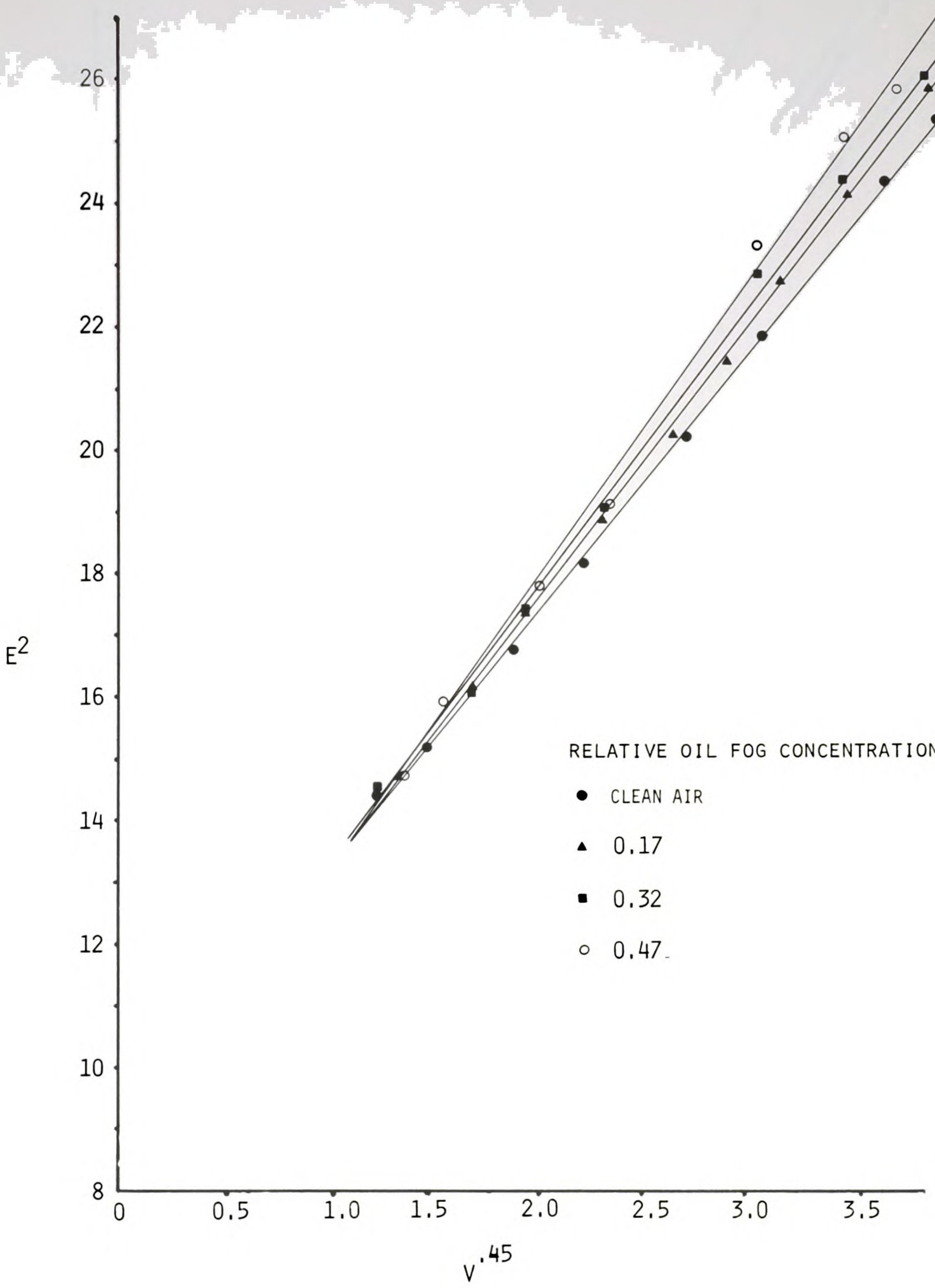

FIGURE 4.1 STRAIGHT WIRE CALIBRATION FOR VARIOUS OIL FOG CONCENTRATIONS -RESISTANCE RATIO=1.8

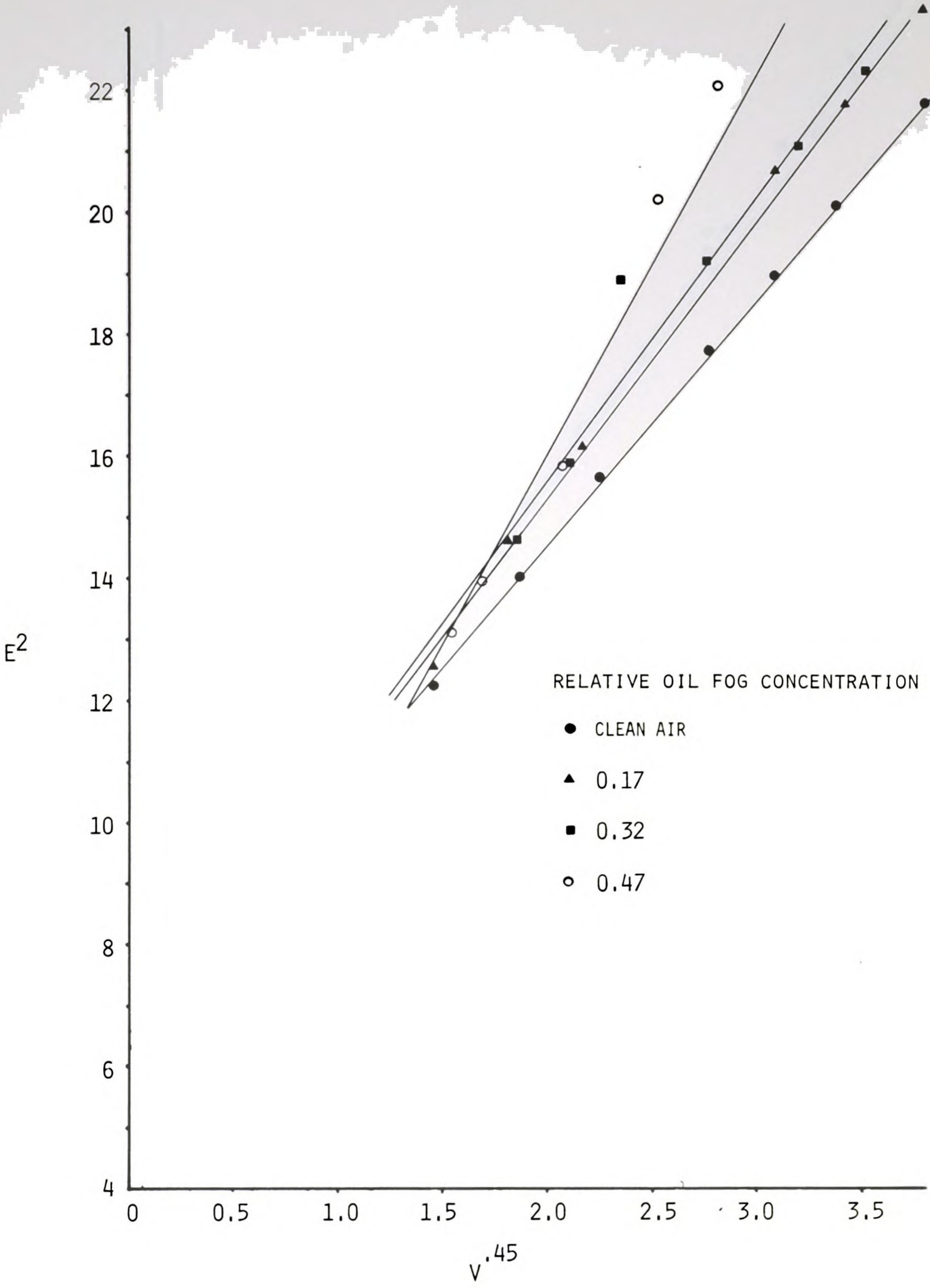

FIGURE 4.2 STRAIGHT WIRE CALIBRATION FOR VARIOUS OIL FOG CONCENTRATIONS-RESISTANCE RATIO=1.6

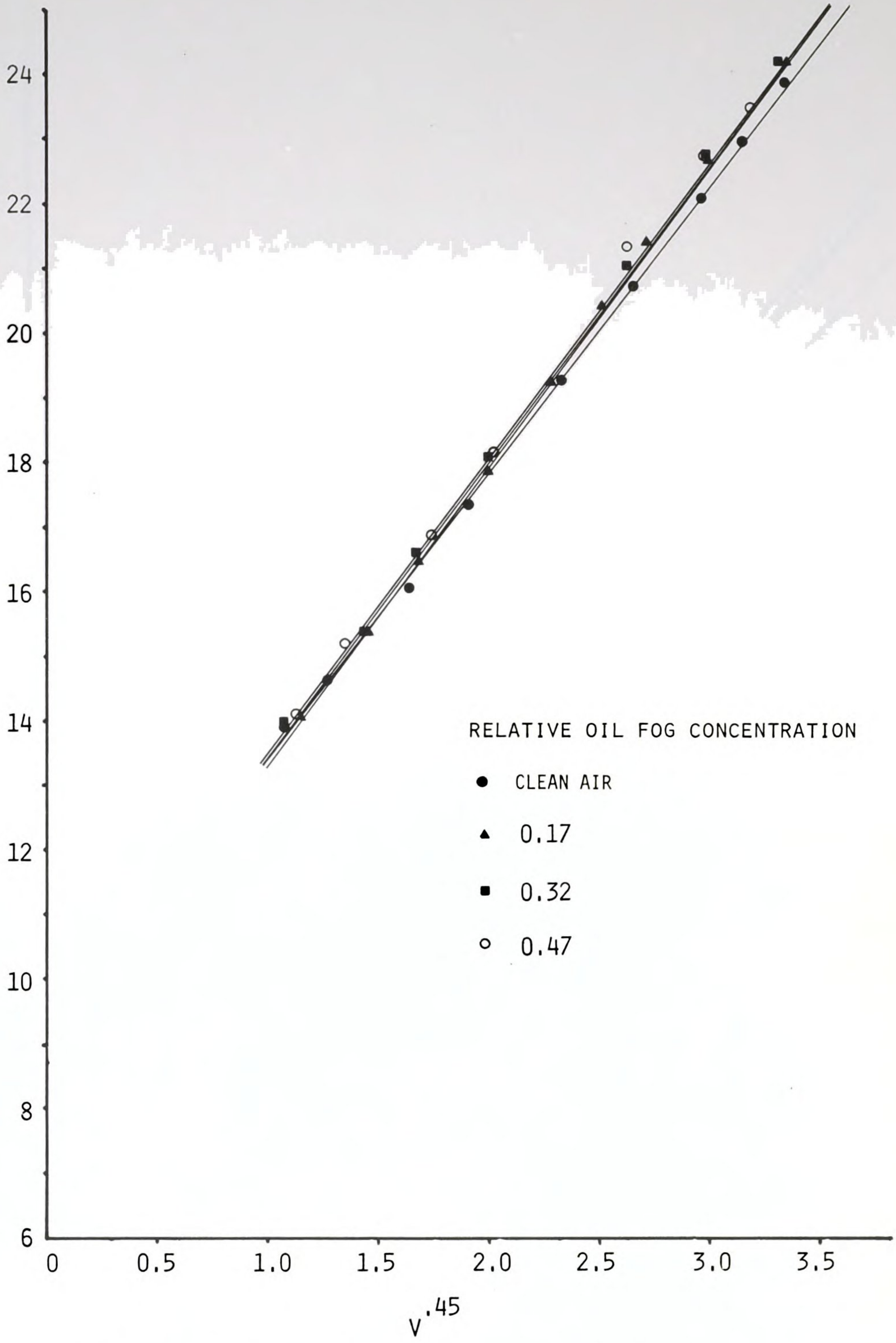

FIGURE 4.3 SLANT WIRE CALIBRATION FOR VARIOUS OIL FOG CONCENTRATIONS -RESISTANCE RATIO=1.8

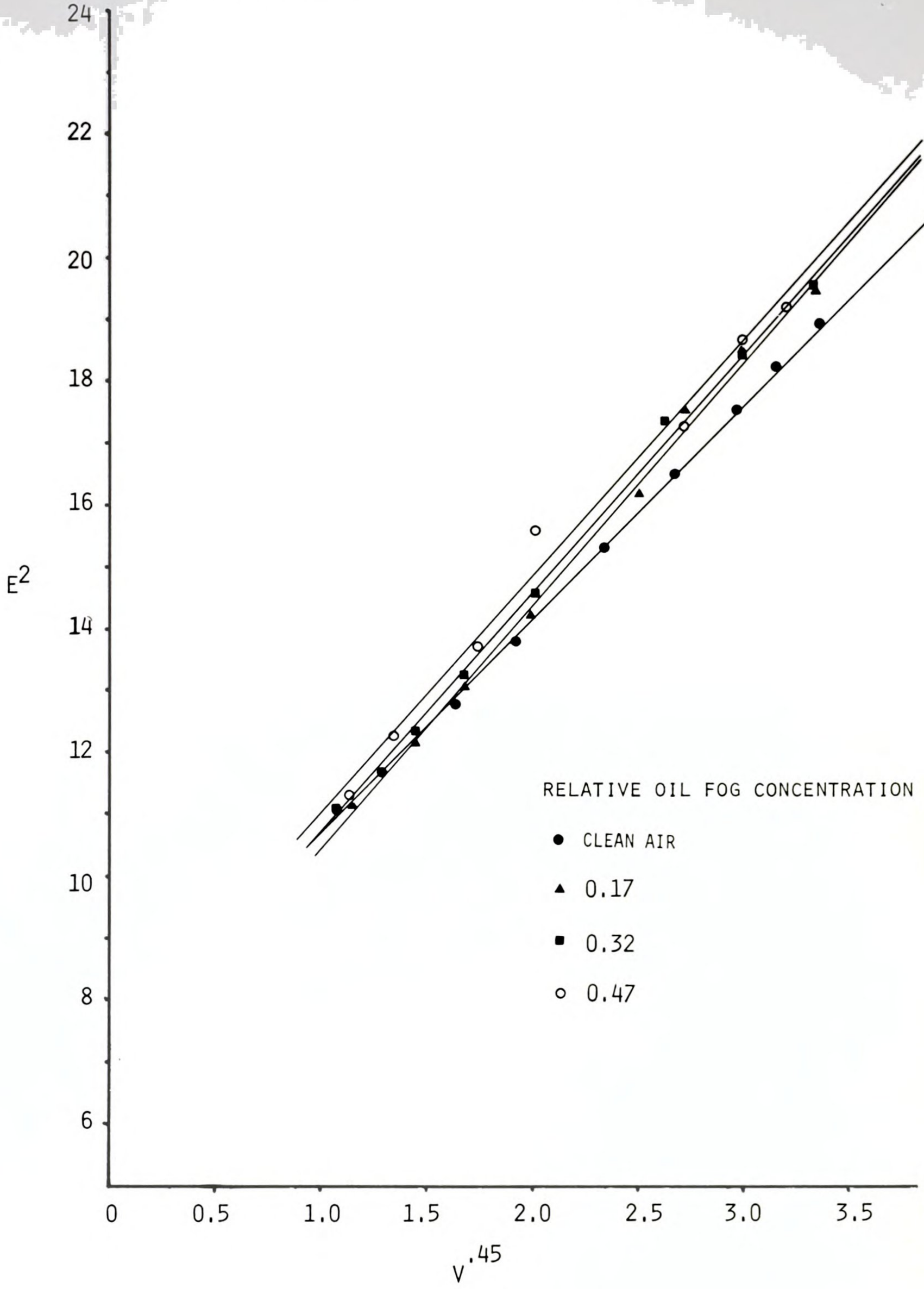

FIGURE 4.4 SLANT WIRE CALIBRATION FOR VARIOUS OIL FOG CONCENTRATIONS -RESISTANCE RATIO=1.6

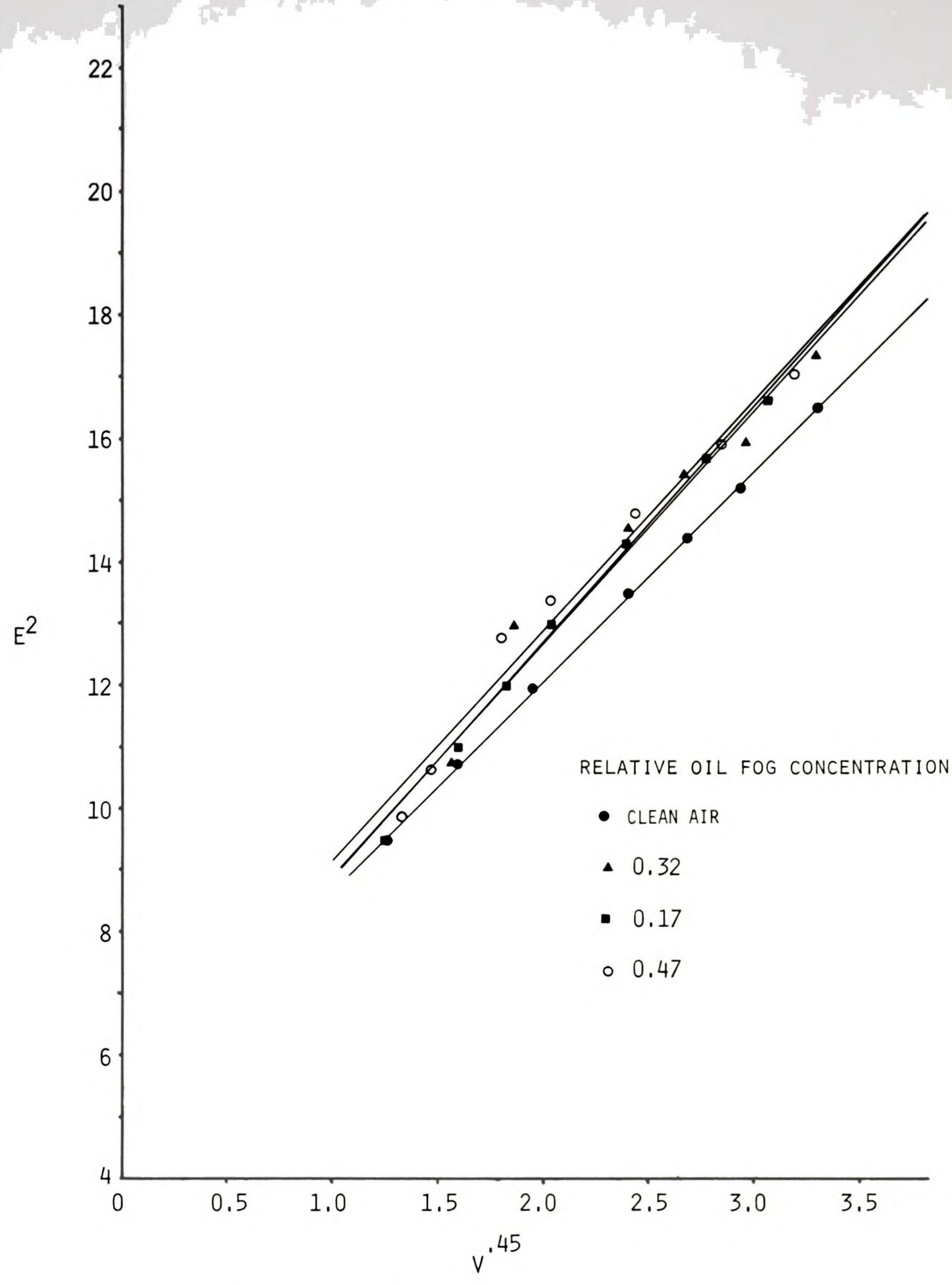

FIGURE 4.5 SLANT WIRE CALIBRATION FOR VARIOUS OIL FOG CONCENTRATIONS -RESISTANCE RATIO=1.45

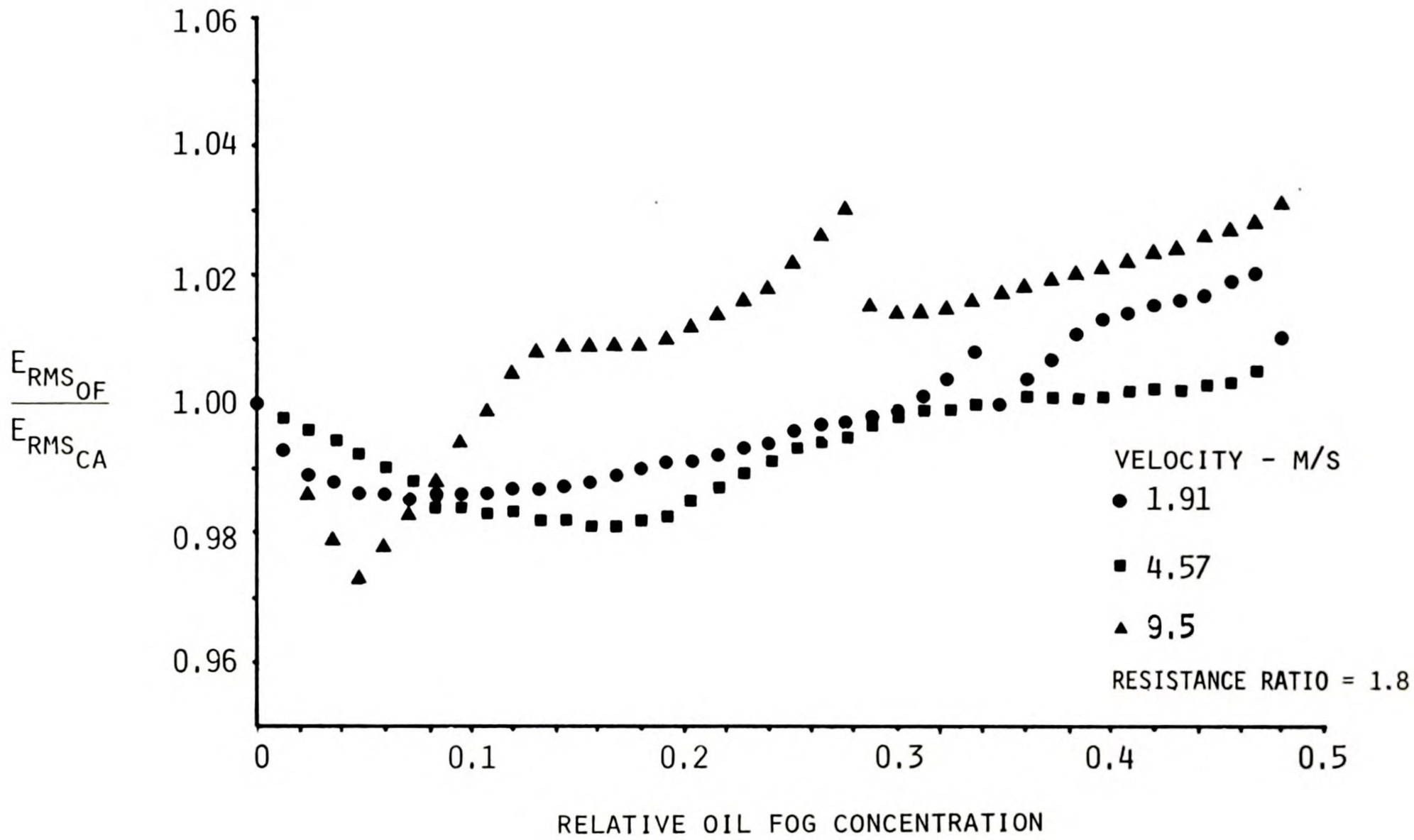

FIGURE 4.6 STRAIGHT WIRE RMS VOLTAGE RESPONSE FOR VARIOUS OIL FOG CONCENTRATIONS

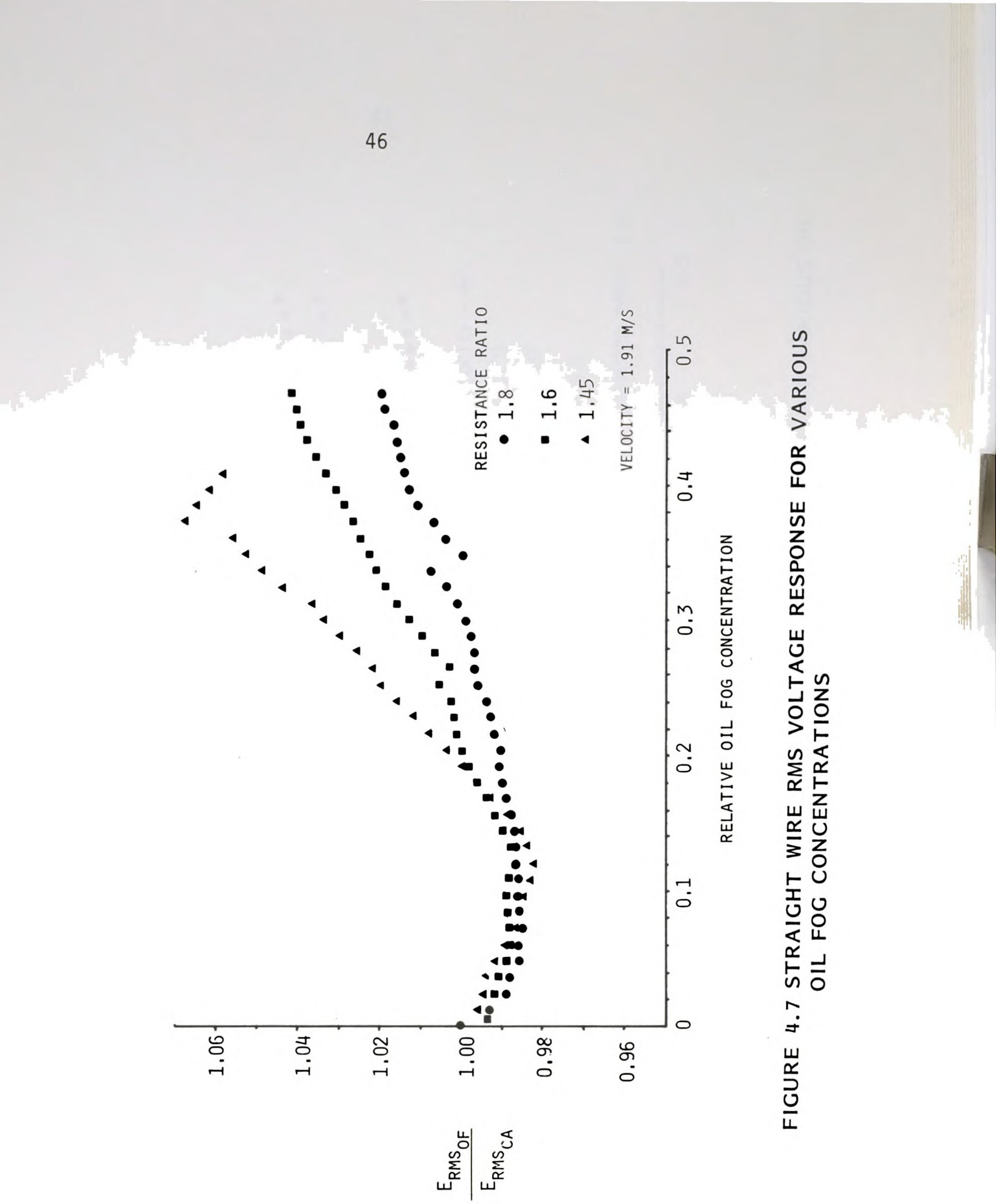

FIGURE 4.7 STRAIGHT WIRE RMS VOLTAGE RESPONSE FOR V
OIL FOG CONCENTRATIONS

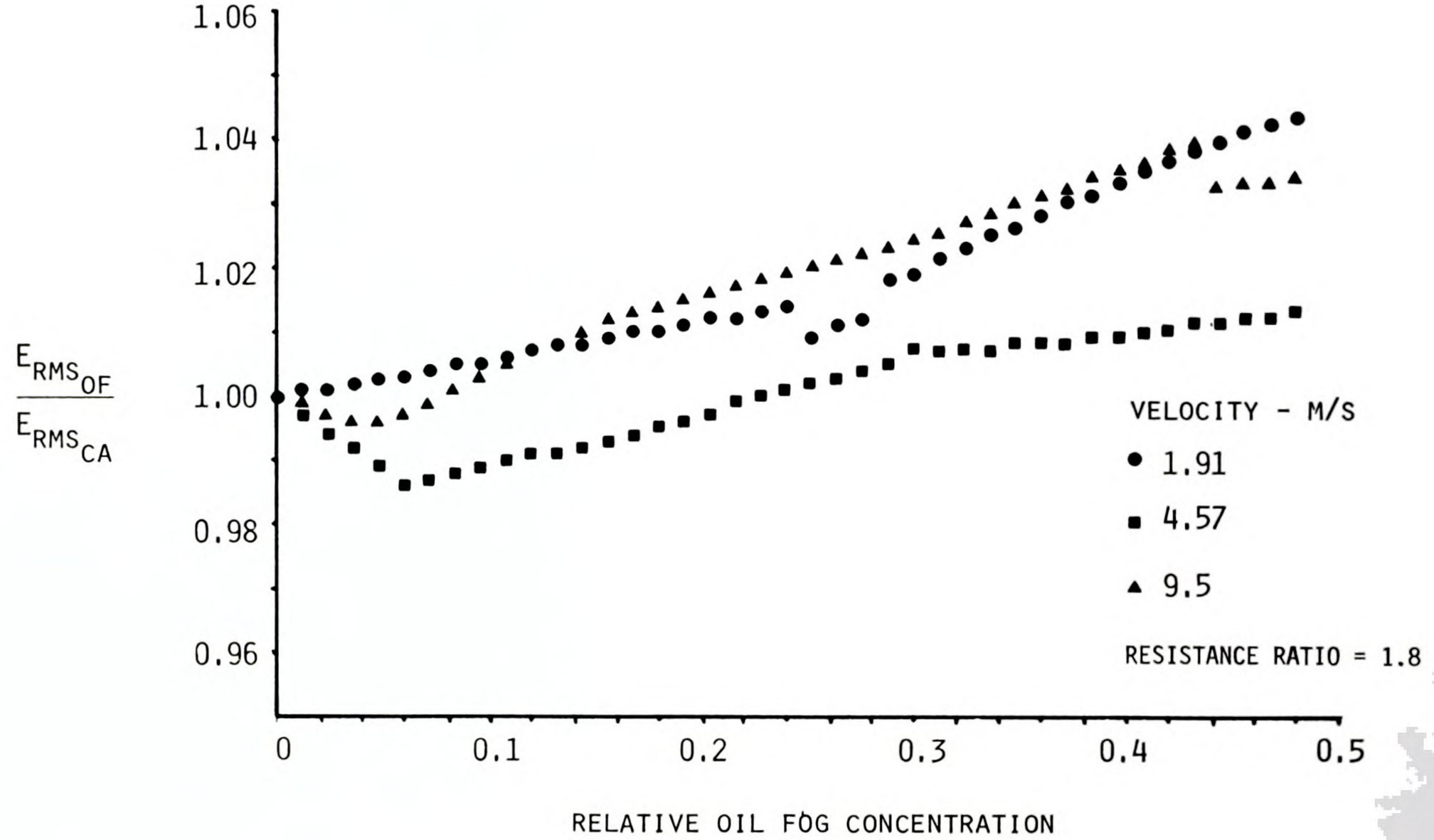

FIGURE 4.8 SLANT WIRE RMS VOLTAGE RESPONSE FOR VARIOUS OIL FOG CONCENTRATIONS

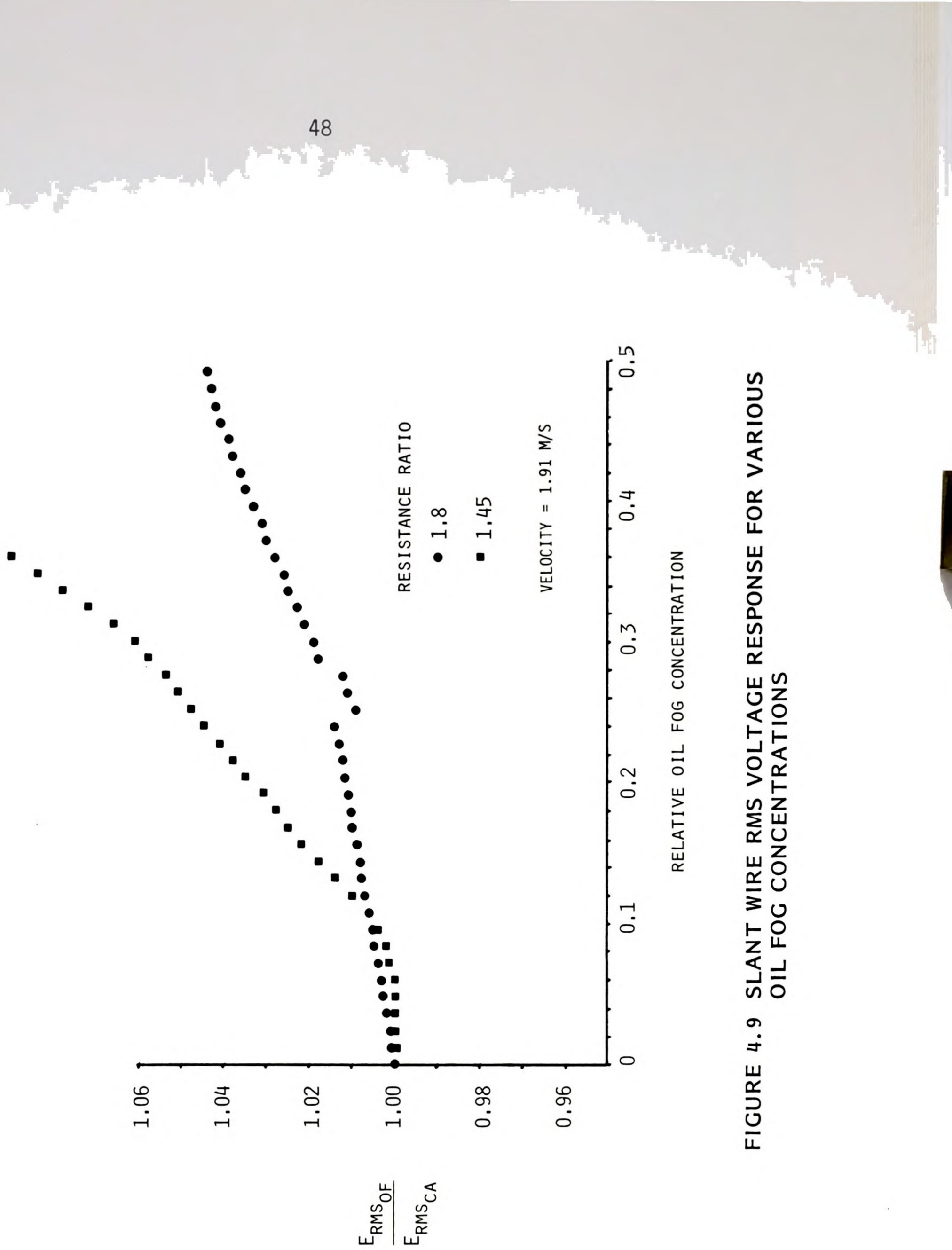

FIGURE 4.9 SLANT WIRE RMS VOLTAGE RESPONSE FOR VARIOUS OIL FOG CONCENTRATIONS

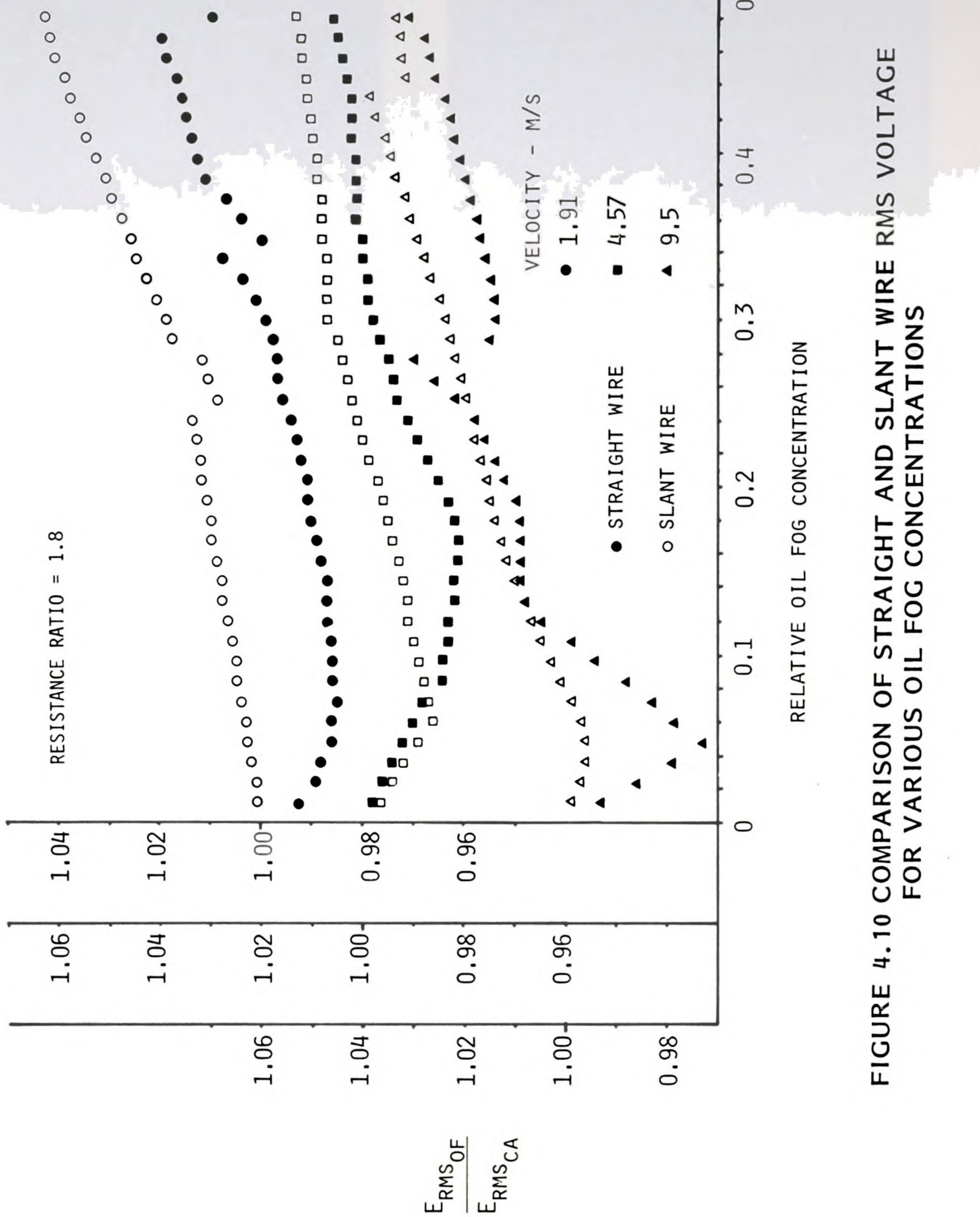

FIGURE 4.10 COMPARISON OF STRAIGHT AND SLANT WIRE RMS VOLTAGE FOR VARIOUS OIL FOG CONCENTRATIONS

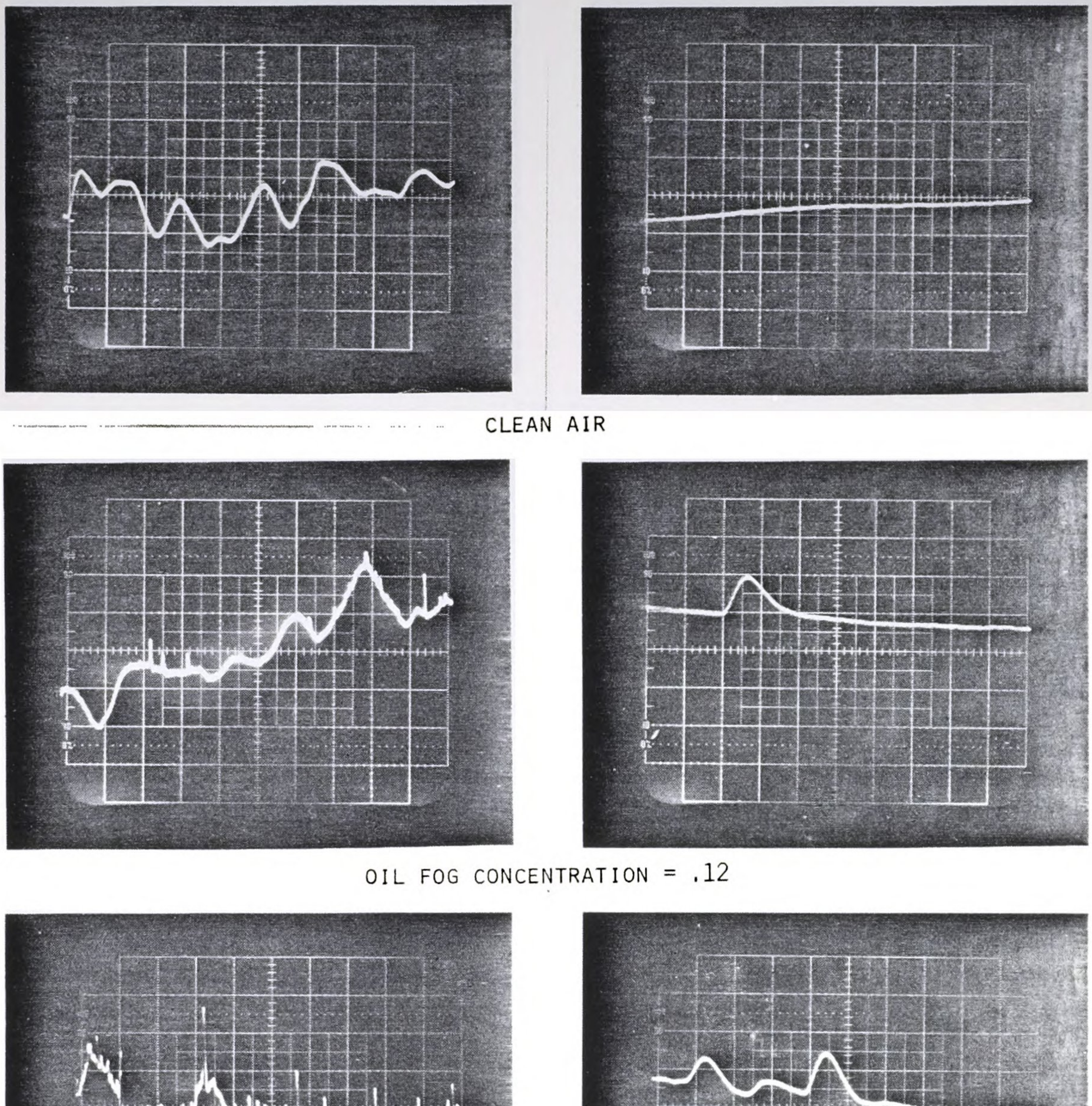

FIGURE 4.11 OSCILLOGRAMS OF SIGNALS FROM A STRAIGHT WIRE OPERATED IN AN OIL FOG AT 1.9 m/s

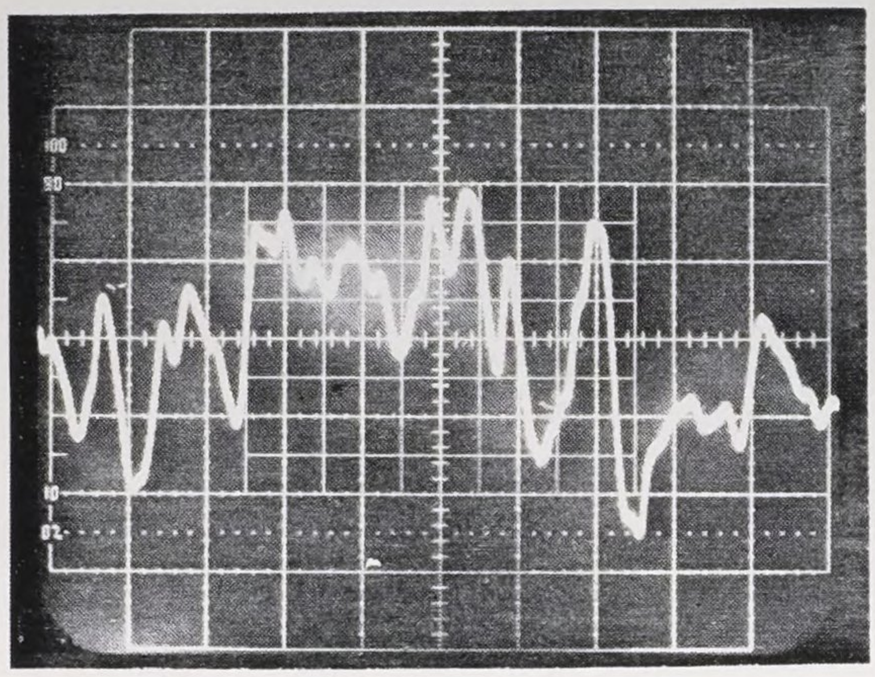

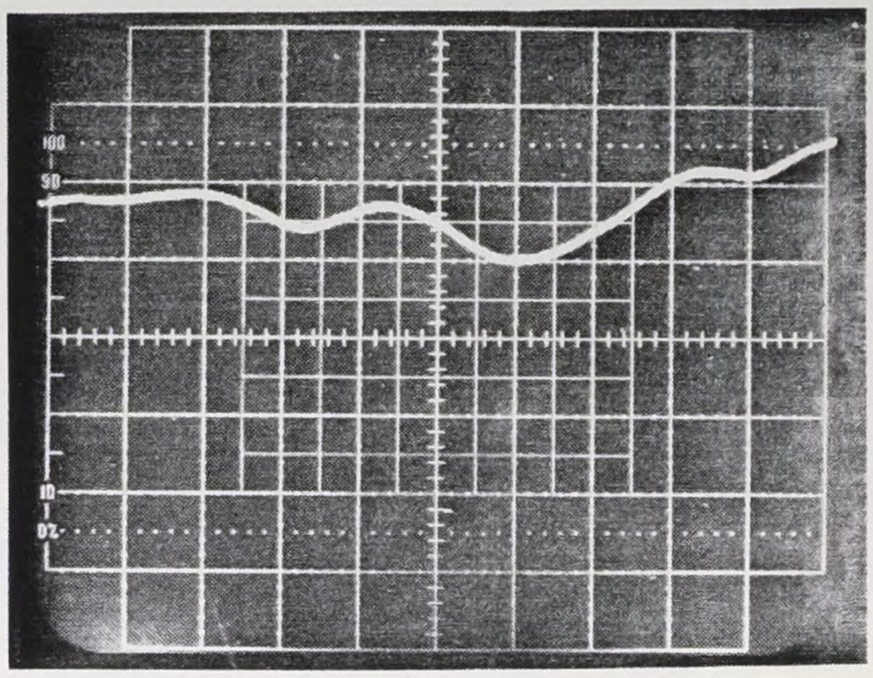

CLEAN AIR

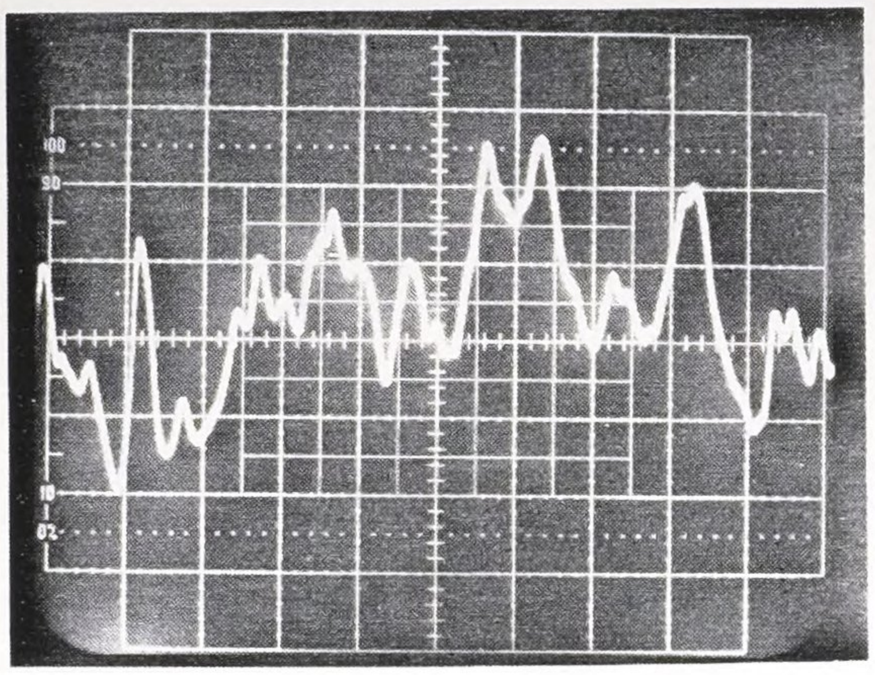

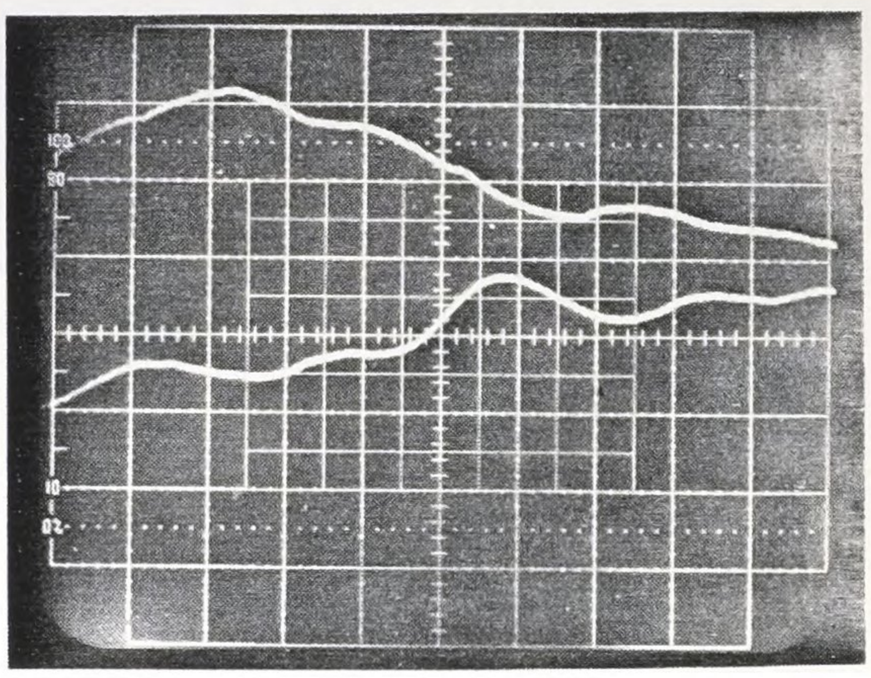

RELATIVE OIL FOG CONCENTRATION = 0.35

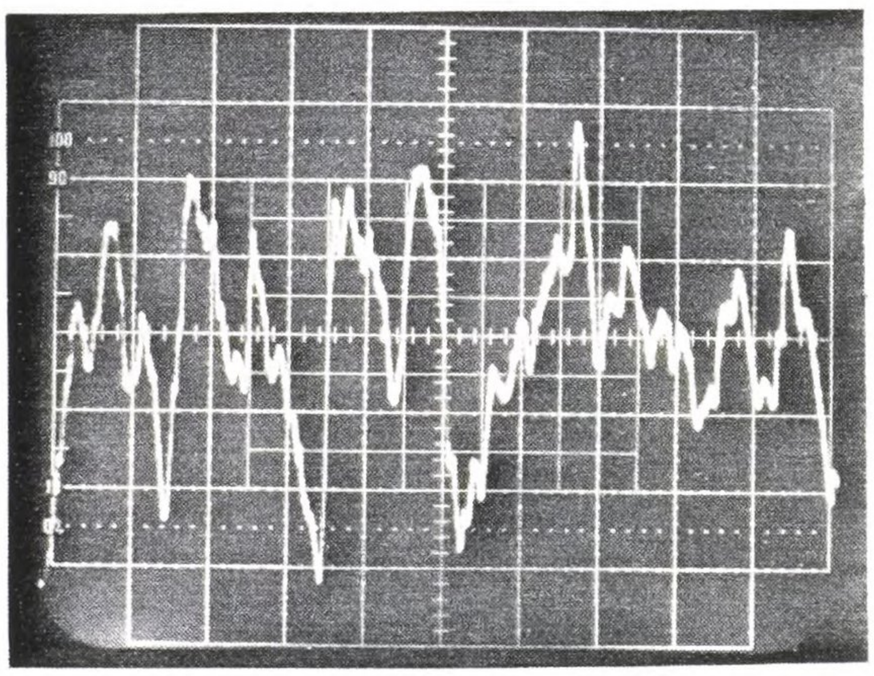

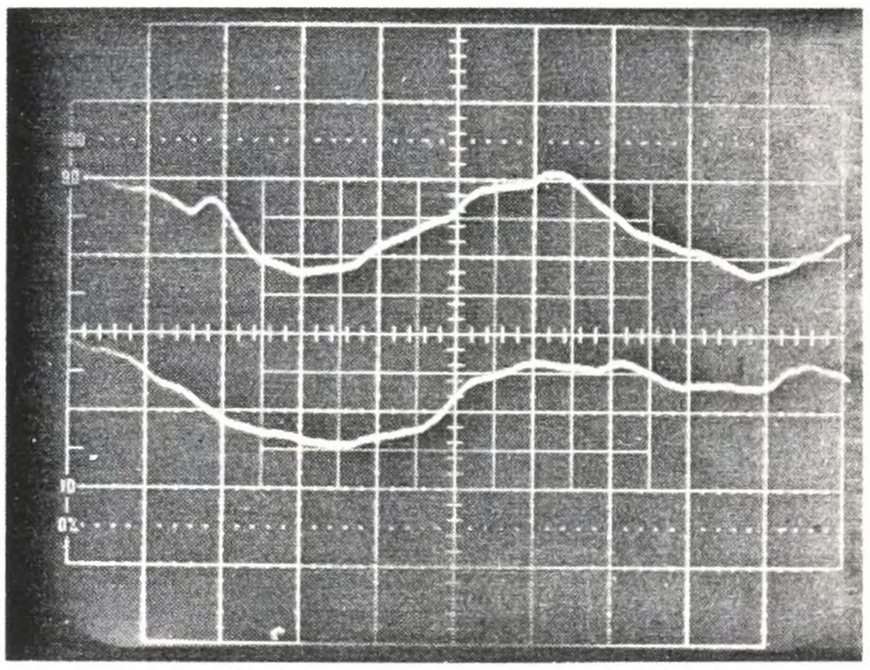

RELATIVE OIL FOG CONCENTRATION = 0.58

VERT SCALE 50 $\frac{MV}{DIV}$

HORS. SCALE 0.5 $\frac{MS}{DIV}$

VERT SCALE 50 $\frac{MV}{DIV}$

HORS. SCALE 50 $\frac{\mu S}{DIV}$

FIGURE 4.12 OSCILLOGRAMS OF SIGNALS FROM A STRAIGHT WIRE OPERATED IN AN OIL FOG AT 9.5 m/s

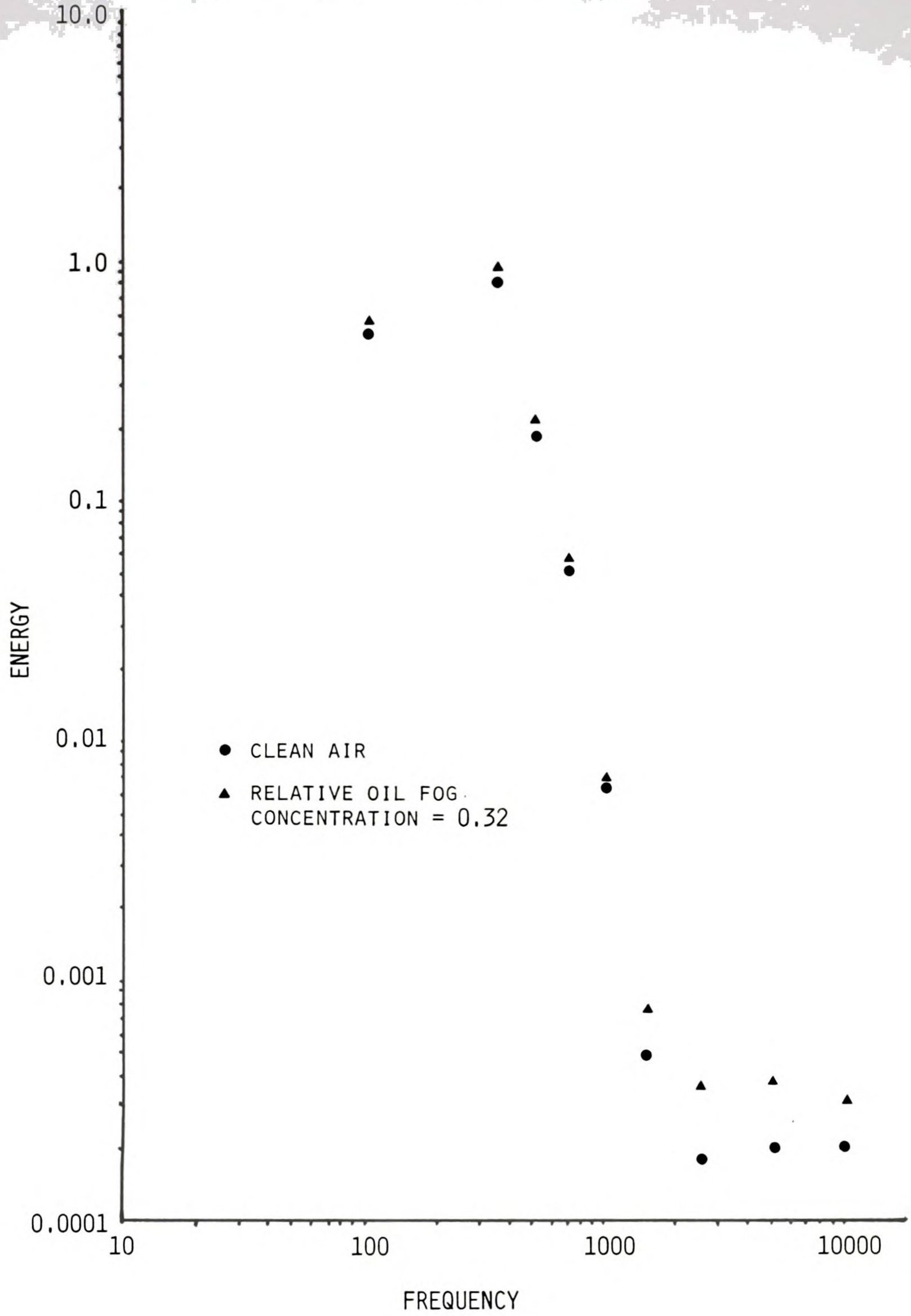

FIGURE 4.13 ENERGY SPECTRA FOR A STRAIGHT WIRE OPERATED IN CLEAN AIR AND AN OIL FOG - VELOCITY=1.9 m/s RESISTANCE RATIO=1.8

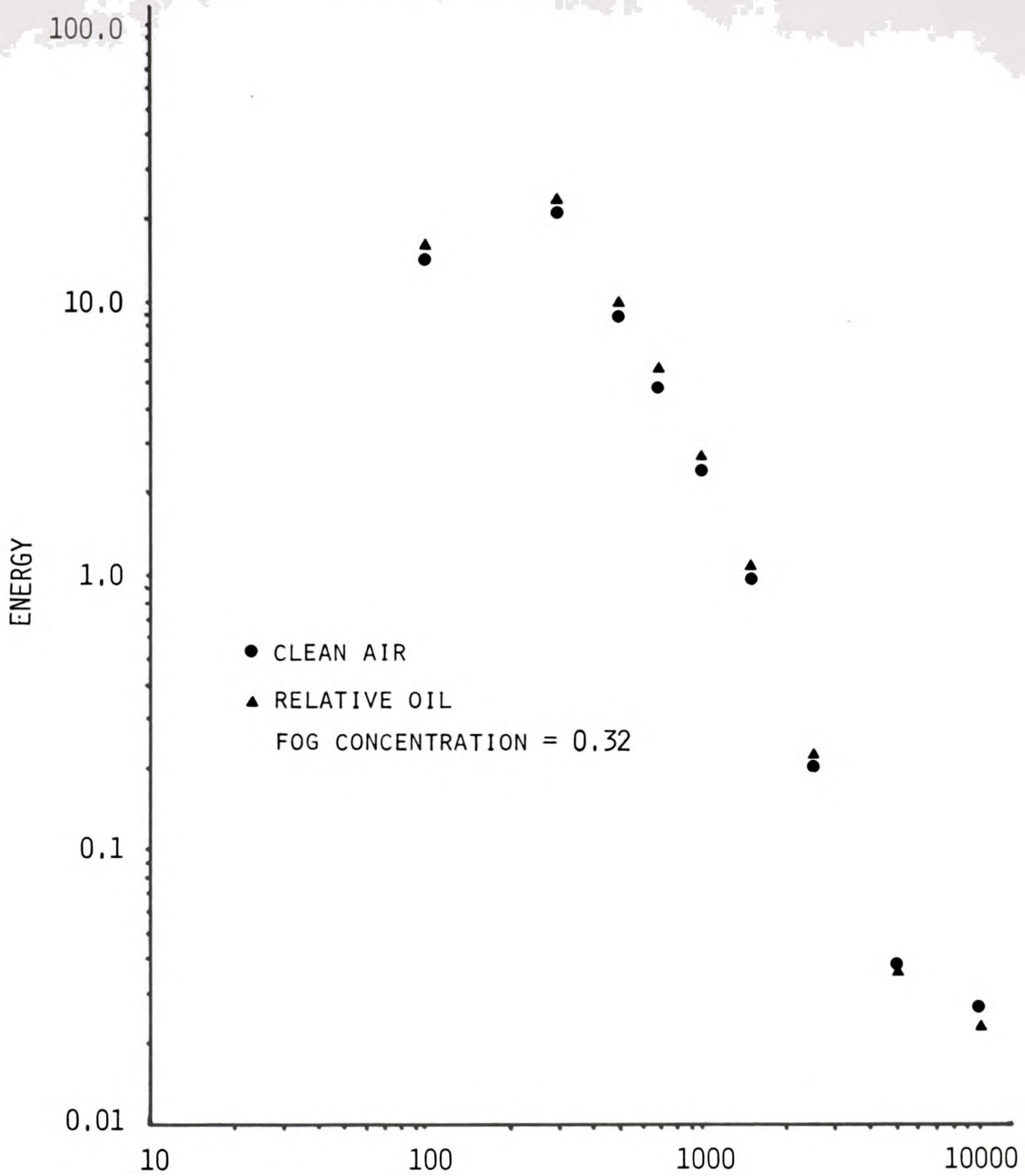

FIGURE 4.14 ENERGY SPECTRA FOR A STRAIGHT WIRE OPERATED IN CLEAN AIR AND AN OIL FOG - VELOCITY=9.0 m/s RESISTANCE RATIO=1.8

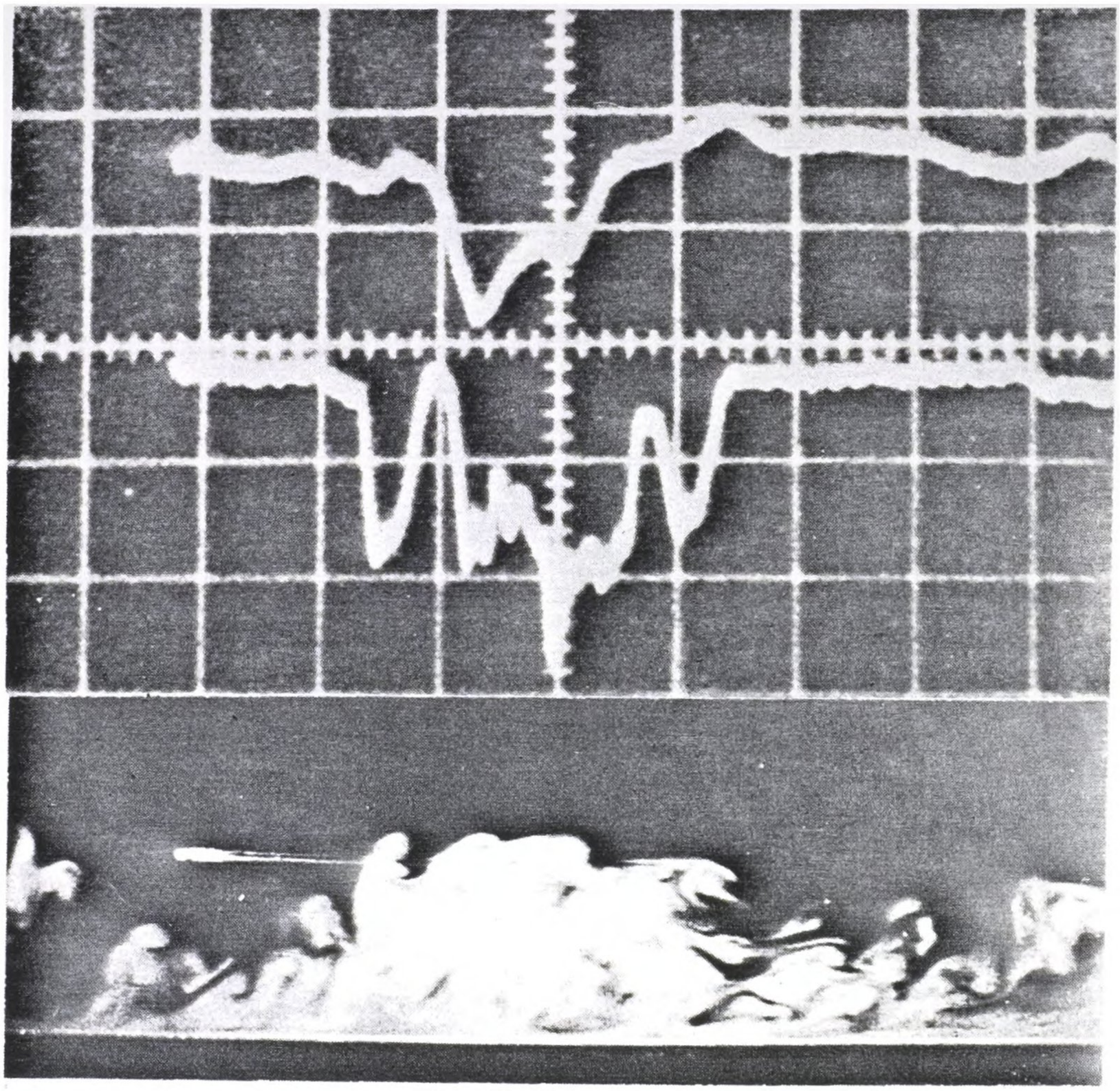

FIGURE 4.15 PHOTOGRAPH OF AN OIL FOG FILLED BOUNDARY LAYER WITH HOT-WIRE AND PHOTOMULTIPLIER TUBE SIGNALS

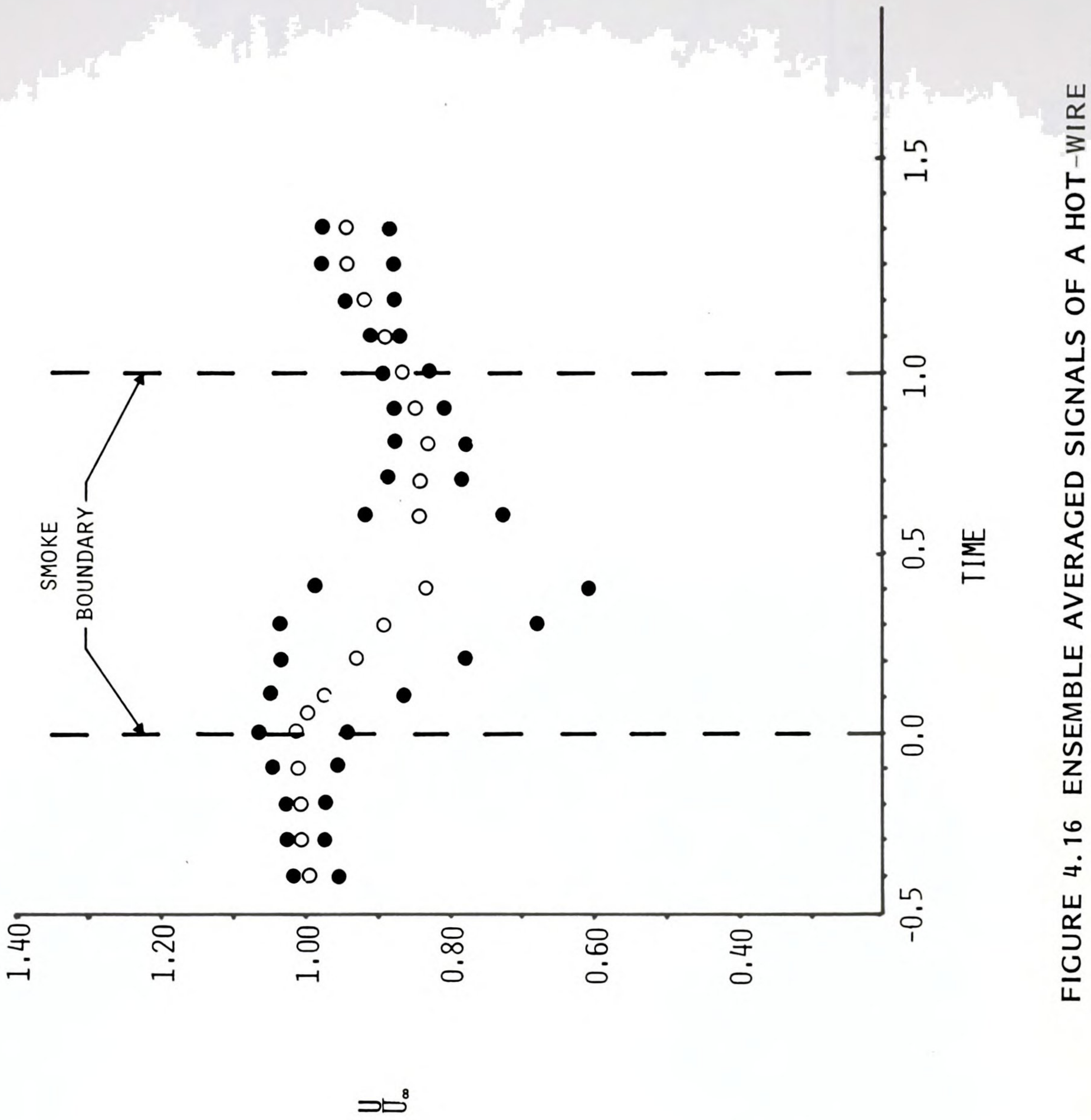

FIGURE 4.16 ENSEMBLE AVERAGED SIGNALS OF A HOT-WIRE ENTERING AND EXITING OIL FOG FILLED REGIONS

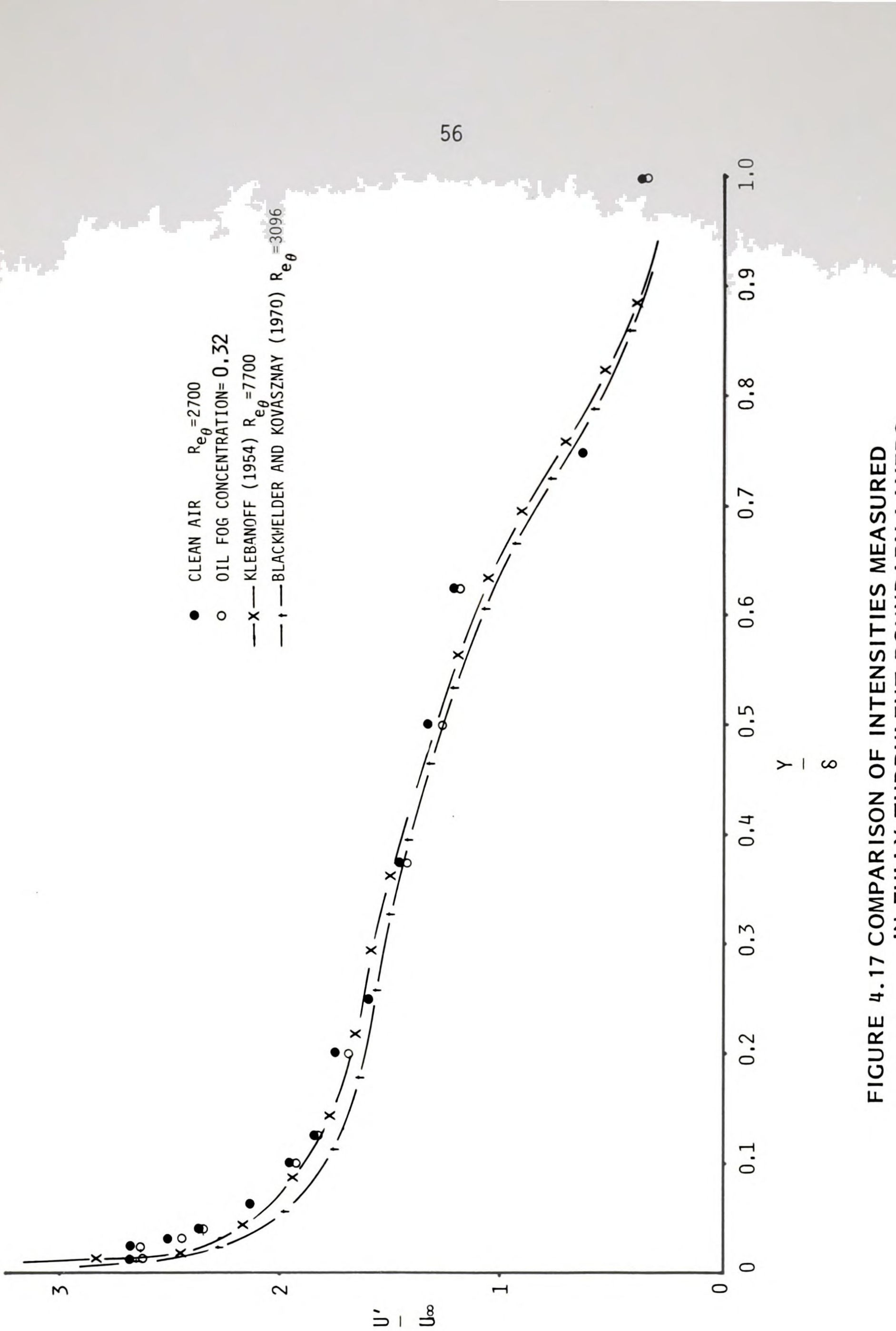

FIGURE 4.17 COMPARISON OF INTENSITIES MEASURED IN FULLY TURBULENT BOUNDARY LAYERS

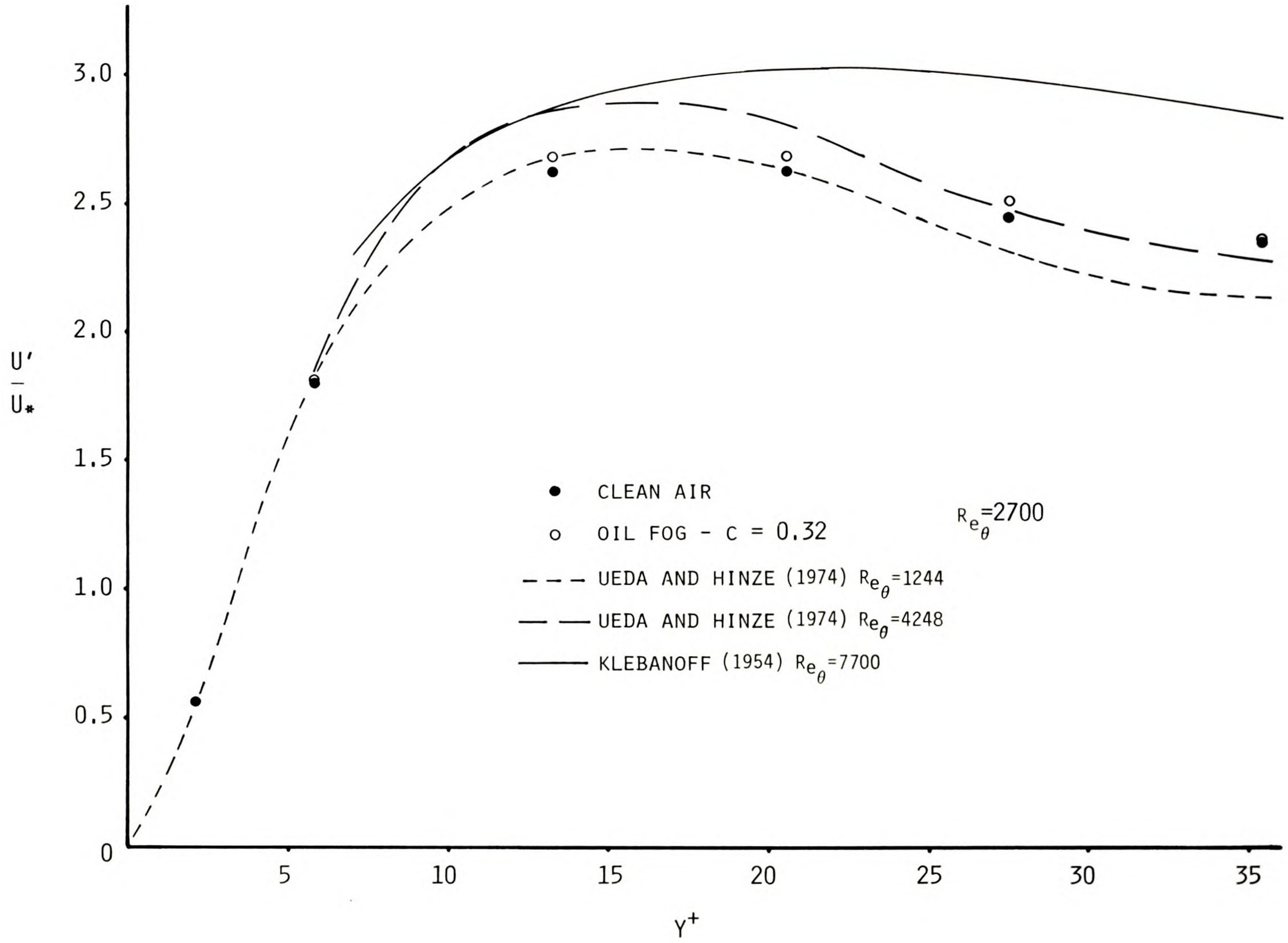

FIGURE 4.18 COMPARISION OF INTENSITIES MEASURED IN THE INNER REGION OF FULLY TURBULENT BOUNDARY LAYERS

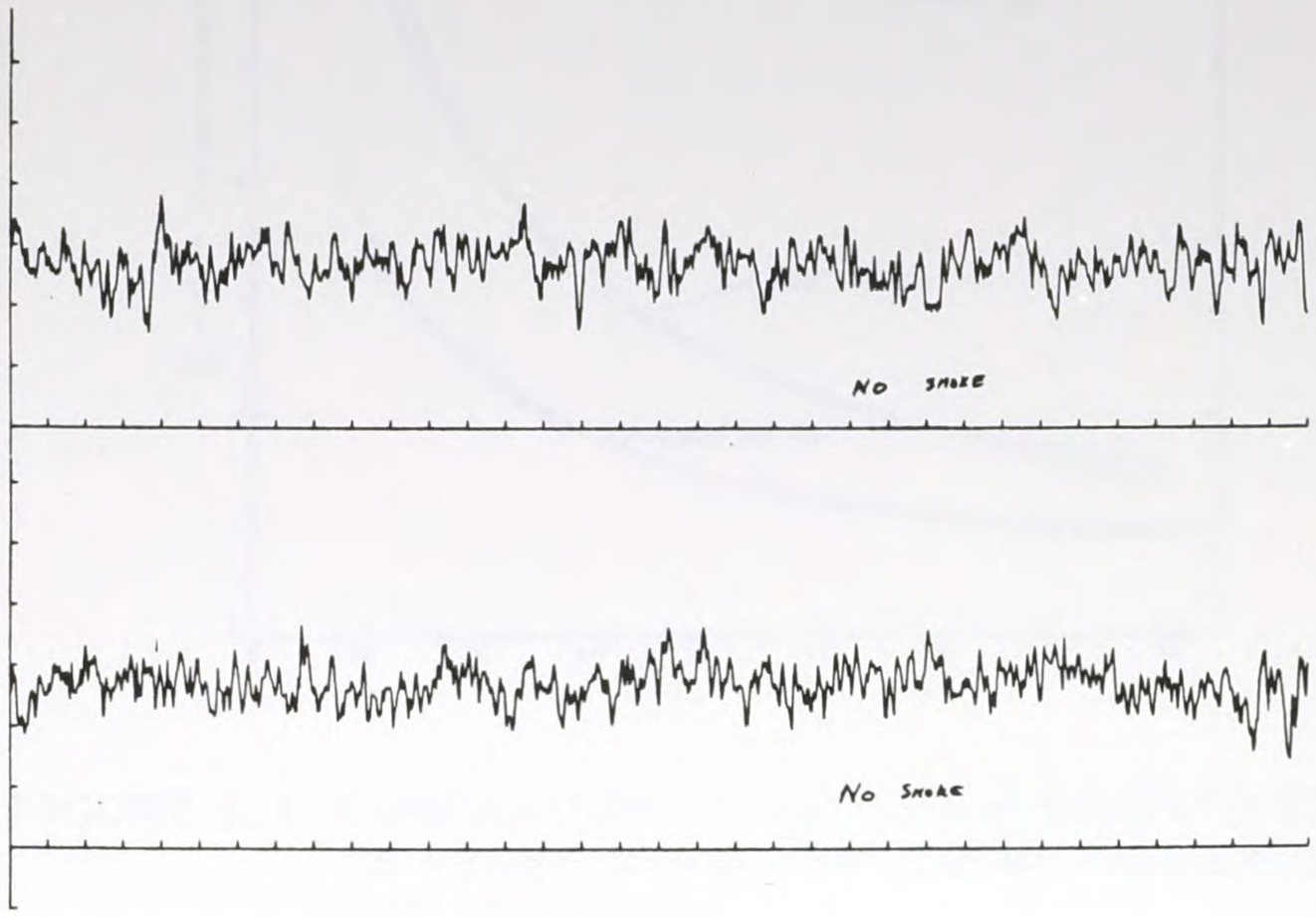

A) CLEAN AIR

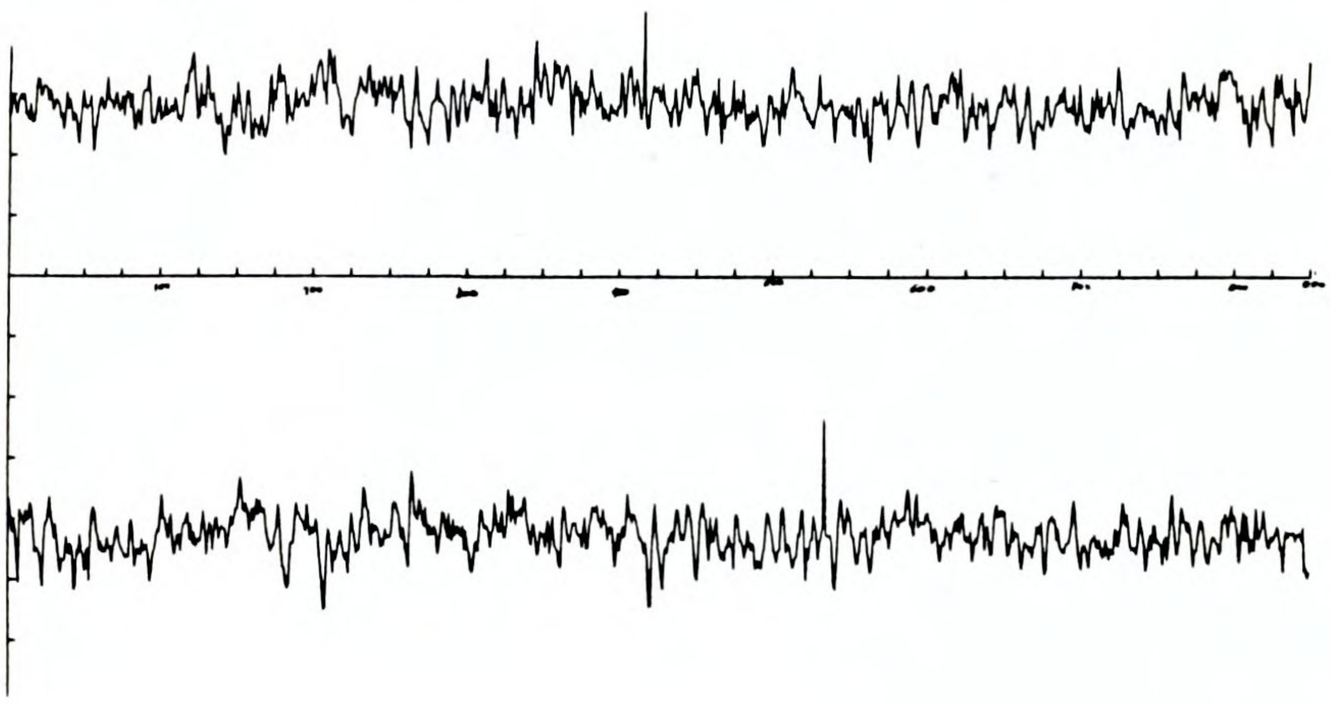

B) RELATIVE OIL FOG CONCENTRATION = 0.35

FIGURE 4.19 DIGITIZED HOT-WIRE VOLTAGE SIGNALS FROM CLEAN AND OIL FOG FILLED BOUNDARY LAYERS

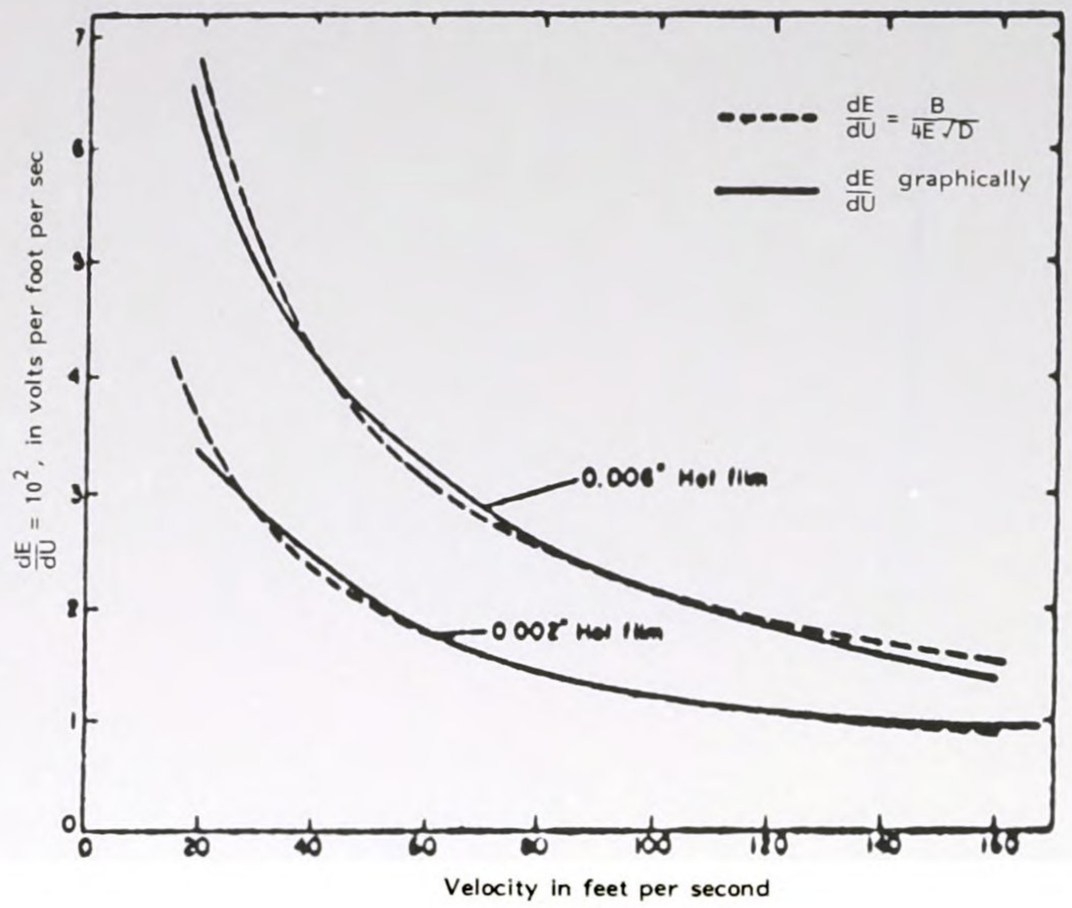

FIGURE 5.1 COMPARISON OF HOT-FILM SENSITIVITY VS PROBE DIAMETER (FROM RICHARDSON AND MCQUIVEY)

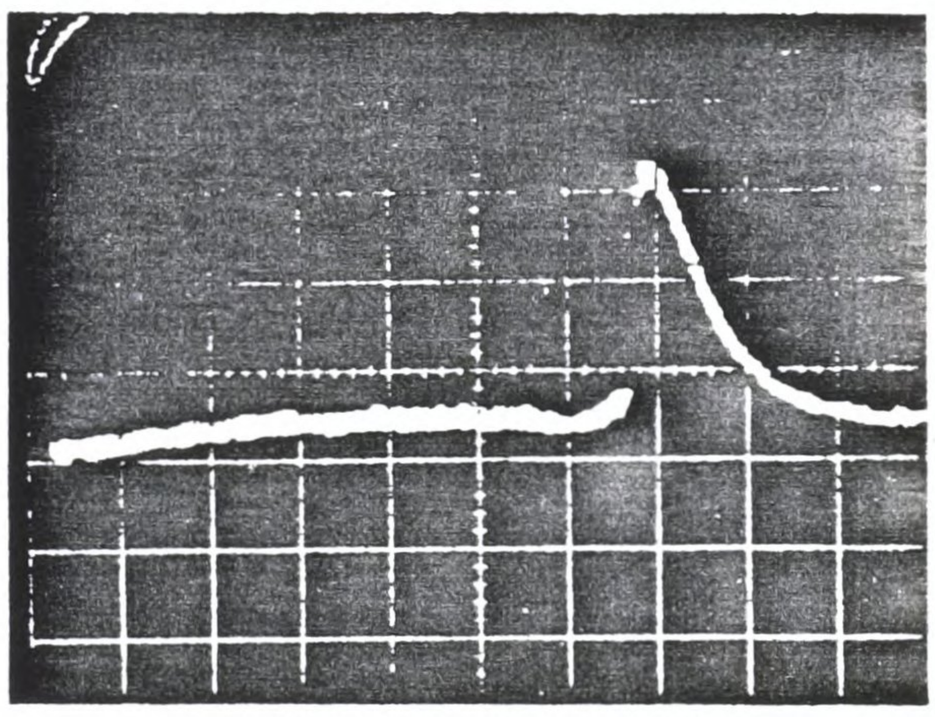

Vertical scale, 0.05 V/division

Horizontal scale, 0.5 msec/division

FIGURE 5.2 16μm DIAMETER SAFFLOWER DROPLET COOLING SIGNAL (FROM GOLDSCHMIDT AND HOUSEHOLDER)

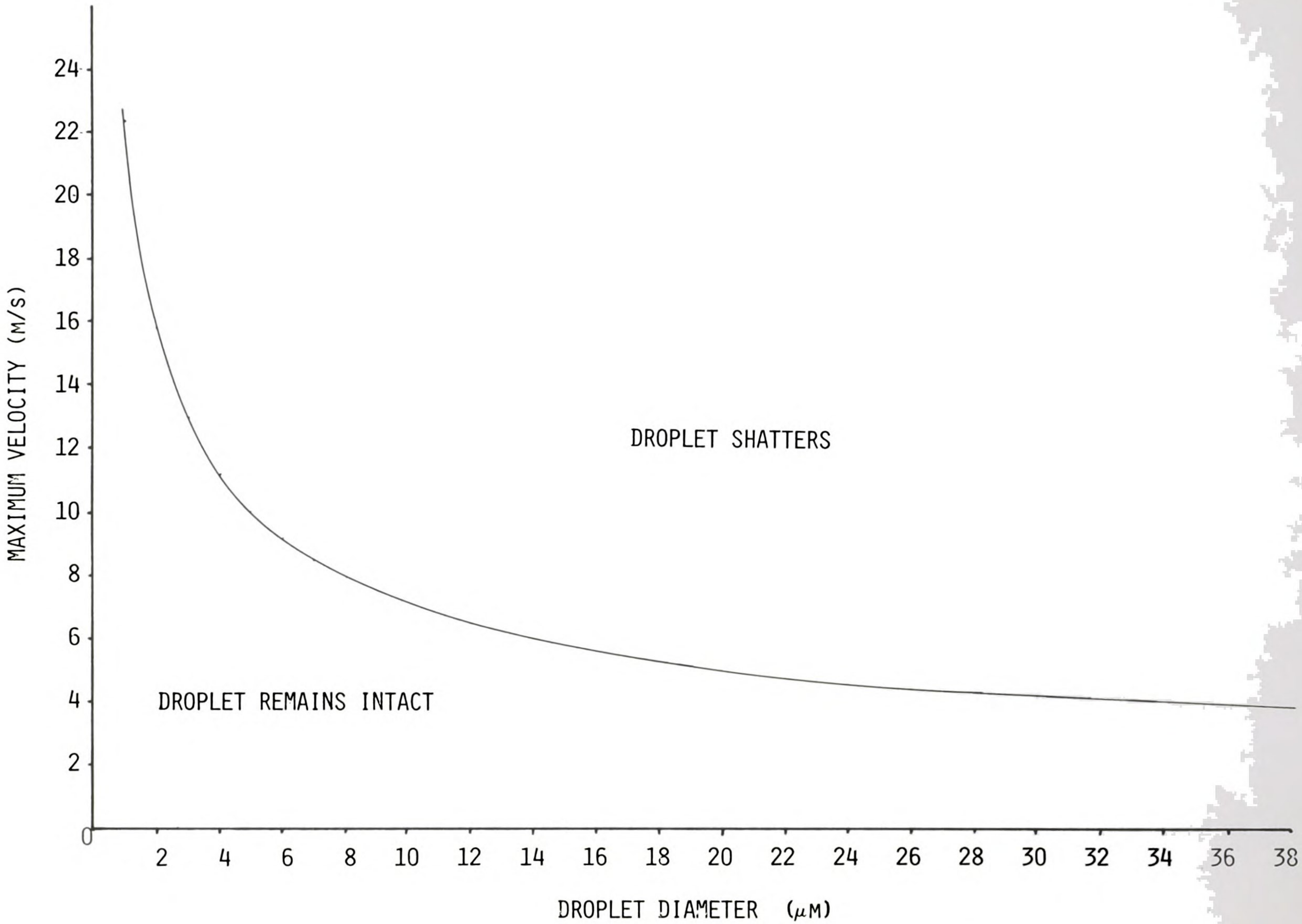

FIGURE 5.3 OIL DROPLET SHATTERING VELOCITY VS DROPLET SIZE

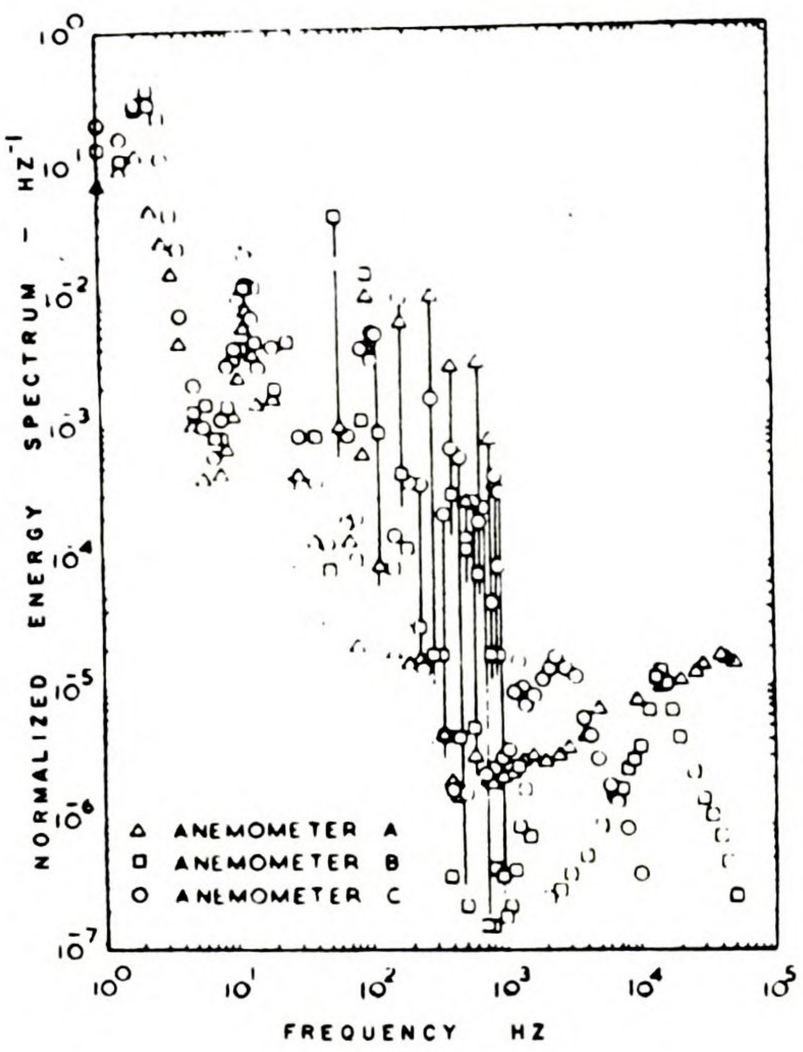

FIGURE 5.4 EFFECT OF DIRT UPON HOT-WIRE ENERGY SPECTRA (FROM MORROW AND KLINE)

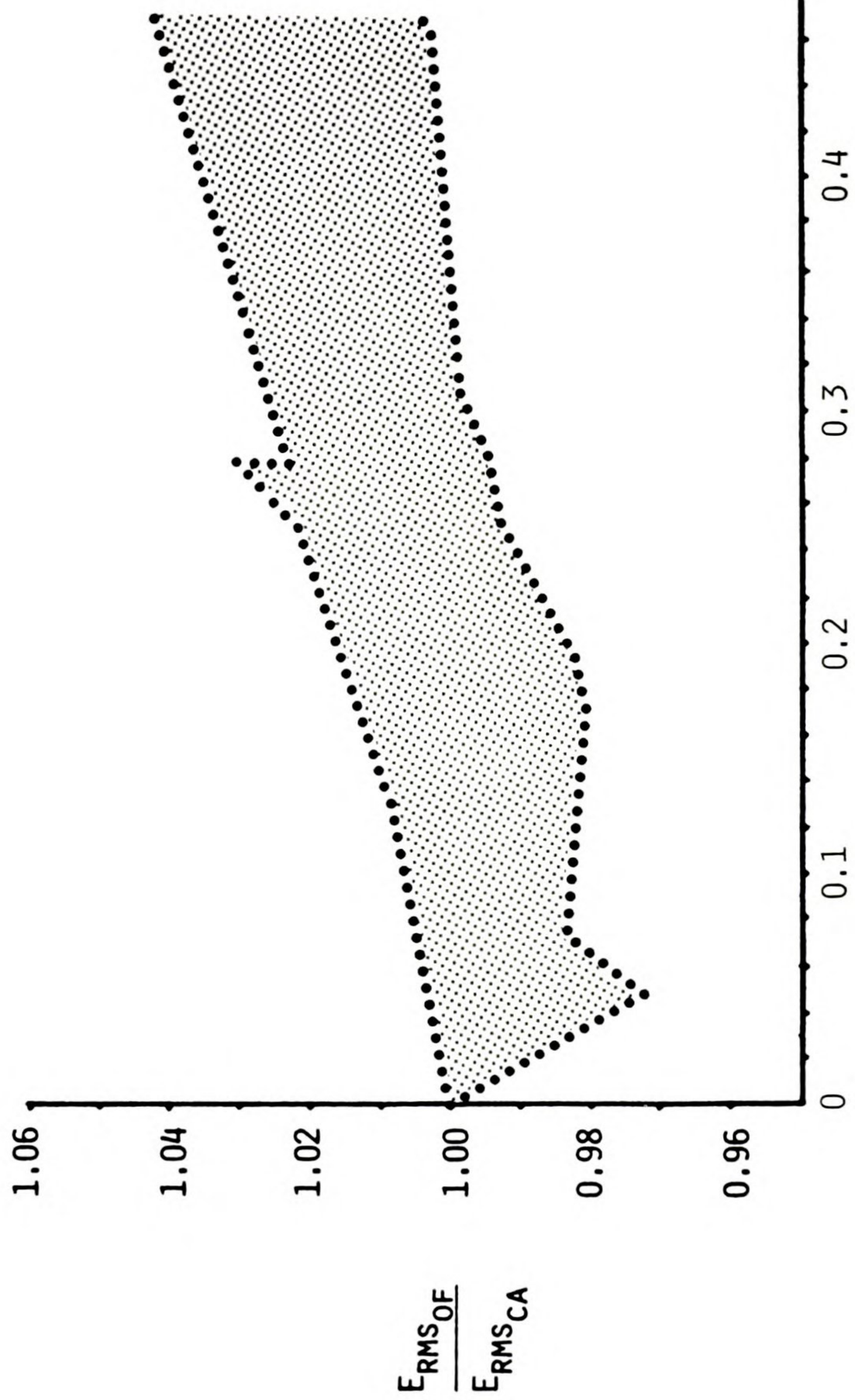

FIGURE 6.1 RMS VOLTAGE ERROR BOUNDS FOR HOT-WIRES OPERATED AT RESISTANCE RATIO=1.8

APPENDIX C

TABLES

Table 3.1

Description	Min.	Typ.	Max	Units
Axial Incidance Response at 770 nm		1.0		$\frac{\mu A}{mW/cm^{(2)}}$
Active Area		2×10^{-3}		$cm^{(2)}$
Flux Responsivity 770 nm		5		$\frac{\mu A}{\mu W}$
Dark Current			6.0	nA
Noise Equivalent Power			8.1×10^{14}	$\frac{W}{\sqrt{Hz}}$
Detectivity	5.6×10^{11}			$\frac{cm \sqrt{Hz}}{W}$
Junction Capacitance			2.0	pF
Package Capacitance				pF
Zero Bias Speed ((Rise, Fall Time)		300		ns
Rev. Bias Speed (Rise, Fall Time)			1	ns
Series Resistance			50	Ω

Data Supplied Courtesy of Hewlett-Packard

WIRE TYPE	R	C	E_o^2	ΔE_o^2	K	ΔK	F
U	1.8	0	9.016		4.223		.9994
		.18	8.711	-.0338	4.469	.0575	.9993
		.32	8.705	-.0343	4.571	.0820	.9982
		.47	8.361	-.0727	4.827	.1430	.9956
	1.6	0	6.527		4.031		.9993
		.18	6.232	-.0449	4.554	.1293	.9953
		.32	6.368	-.0237	4.639	.1500	.9664
		.47	3.621	-.4450	6.637	.5460	.9857
X	1.8	0	8.986		4.446		.9994
		.18	8.676	-.0345	4.679	.0524	.9998
		.32	8.856	-.0144	4.639	.0435	.9994
		.47	8.935	-.0056	4.631	.0418	.9980
	1.6	0	7.163		3.530		.9992
		.18	6.483	-.0950	3.969	.1242	.9961
		.32	6.827	-.0470	3.898	.1042	.9965
		.47	7.166	.0004	3.861	.0937	.9895
	1.45	0	5.192		3.419		.9997
		.18	5.115	-.0148	3.763	.1006	.9745
		.32	5.011	-.0348	3.816	.1163	.9963
		.47	5.369	.0340	3.746	.0957	.9744

TABLE 4.1 COLLIS AND WILLIAMS PARAMETERS FOR HOT-WIRE CALIBRATIONS (M CONSTANT)

WIRE TYPE	R	C	E_o^2	ΔE_o^2	K	ΔK	M	ΔM	STD. DEVIAT.
U	1.8	0	5.4820		3.843		.4743		.03827
		.18	5.0050	-.0503	4.234	.1157	.4636	-.0225	.07117
		.32	5.162	-.0338	4.201	.0568	.4714	-.0062	1.2415
		.47	8.6973	-.0828	4.555	.1987	.4648	-.0200	1.6261
	1.6	0	6.239		4.259		.4367		0.3712
		.18	4.884	-.2173	5.759	.4183	.3965	-.0921	3.8067
		.32	5.825	-.0664	5.481	.3436	.4004	-.0832	4.3756
		.47	2.752	-.5590	6.925	.6495	.4246	-.0276	3.4414
X	1.8	0	5.473		4.0145		.4777		0.3757
		.18	8.729	-.0785	4.629	.1852	.4531	-.0516	0.3307
		.32	9.231	-.0256	4.311	.0815	.4703	-.0155	0.4631
		.47	8.732	-.0783	4.810	.2513	.4397	-.0756	1.2634
	1.6	0	7.634		3.123		.4839		0.4453
		.18	6.657	-.1228	3.782	.2408	.4632	-.0427	1.6341
		.32	7.005	-.0824	3.745	.2321	.4608	-.0476	1.5540
		.47	6.048	-.2082	4.844	.7348	.3907	-.1926	1.5250
	1.45	0	5.255		3.414		.4475		0.1716
		.18	4.739	-.0981	4.779	.5545	.3592	-.1972	5.8786
		.32	4.798	-.0870	3.991	.1817	.4383	-.0205	1.0064
		.47	3.829	-.2713	5.064	.6183	.3741	-.1640	2.1982

TABLE 4.2 COLLIS AND WILLIAMS PARAMETERS FOR HOT-WIRE CALIBRATIONS (M VARIABLE)

WIRE TYPE	R	C	1.5 m/s dE/dV	1.5 m/s PERCENT CHANGE	3.0 m/s dE/dV	3.0 m/s PERCENT CHANGE	6.1 m/s dE/dV	6.1 m/s PERCENT CHANGE	9.1 m/s dE/dV	9.1 m/s PERCENT CHANGE	12.2 m/s dE/dV	12.2 m/s PERCENT CHANGE	15.2 m/s dE/dV	PERCENT CHANGE	18.3 m/s dE/dV	18.3 m/s PERCENT CHANGE	19.8 m/s dE/dV	19.8 m/s PERCENT CHANGE
U	1.8	0	.1939		.1270		.0817		.0630		.0522		.0449		.0397		.0377	
		.18	.2080	7.28	.1345	5.94	.0860	5.22	.0656	4.17	.0541	3.77	.0466	3.65	.0410	3.31	.0387	2.61
		.32	.2056	8.12	.1362	7.24	.0873	6.83	.0669	6.25	.0551	5.66	.0476	5.84	.0420	5.79	.0397	5.22
		.47	.2238	15.40	.1453	14.47	.0915	12.05	.0699	10.94	.0574	10.05	.0495	10.22	.0436	9.92		
	1.6	0	.2175		.1368		.0850		.0640		.0522		.0446		.0390		.0371	
		.18	.2589	19.00	.1565	14.39	.0938	10.42	.0692	8.21	.0558	6.92	.0472	5.88	.0410	5.04	.0387	4.42
		.32	.2428	11.61	.1483	8.39	.0896	5.41	.0666	4.10	.0538	3.14	.0456	2.21				
		.47	.3474	59.73	.2080	52.04	.1237	45.56	.0909	42.05	.0732	40.25	.0617	38.24	.0535	14.29		
X	1.8	0	.2031		.1329		.0856		.0659		.0545		.0469		.0417		.0394	
		.18	.2198	8.24	.1407	5.93	.0889	3.83	.0676	2.49	.0554	1.81	.0476	1.40	.0420	0.79	.0397	0.83
		.32	.2129	4.85	.1381	3.95	.0886	3.45	.0679	2.99	.0561	3.01	.0482	2.80	.0427	2.36	.0404	2.50
		.47	.2192	7.92	.1391	4.69	.0873	1.92	.0659	0.00	.0541	-0.60	.0463	-1.40	.0407	-2.36		
	1.4	0	.1795		.1181		.0764		.0591		.0489		.0423		.0374		.0354	
		.18	.2080	15.90	.1335	13.06	.0846	10.73	.0643	8.89	.0528	8.05	.0138	6.98	.0400	7.02	.0377	6.48
		.32	.2021	12.61	.1299	10.00	.0823	7.73	.0151	6.11	.0515	5.37	.0443	4.65	.0390	4.39	.0367	3.70
		.47	.2136	19.01	.1306	10.56	.0791	3.34	.0587	-0.56	.0476	-2.68	.0400	-5.43	.0351	-6.14		
	1.45	0	.1978		.1250		.0784		.0591		.0486		.0413		.0364		.0344	
		.18	.2041	3.15	.1220	-2.36	.0722	-7.95	.0531	-10.00	.0427	-12.16	.0358	-13.49	.0312	-14.41	.0292	-15.24
		.32	.2228	12.60	.1391	11.29	.0860	9.62	.0643	8.89	.0525	8.11	.0446	7.94				
		.47	.2329	17.74	.1388	11.02	.0823	5.02	.0604	2.22	.0482	-0.68	.0407	-1.59	.0354	-2.70		

TABLE 4.3 HOT-WIRE SENSITIVITY VS VELOCITY

APPENDIX D

ESTIMATE OF FORCE REQUIRED TO SHATTER DROPLETS

$$F = \pi \sigma d$$

The momentum of the drop is

$$= mv = \rho V v$$

$$= \rho (4/3 \pi R^3) v$$

$$= \rho (4/3 \pi \frac{d^3}{8} v$$

$$= \rho \pi \frac{d^3}{6} v$$

Rate of change of momentum is

$$\frac{dM}{dt} = \frac{\Delta M}{\Delta t}$$

The time required for the drop to be brought to rest is determined by the distance the drop travels before being brought to rest, which is proportional to the drop diameter, i.e., divided by the average drop velocity. Δt is then

$$\frac{nd}{v/2}$$

The rate of Momentum change then becomes

$$\frac{\rho \tau \frac{d^3}{6} v - 0}{\frac{nd}{v/2}} = \frac{\rho \pi d^2 v^2}{12n}$$

Equating this with the surface tension force gives

$$v_{MAX} = \frac{12\ n\ \sigma}{\rho d}$$

APPENDIX E

COMPUTER PROGRAMS

```
// JOB


// FOR CALFT
*NONPROCESS PROGRAM
*ONE WORD INTEGERS
*IOCS(CARD,1443 PRINTER)
C
C*FINDS BEST EO**2,K,M FOR EACH WIRE, FOR EACH GAMMA.
C COMPUTES VELOCITY GIVEN THESE PARAMS, AND ITS ST DEV FROM TRUE VEL.
C OPTIONALLY PUNCHES EO**2,K,M.
C
C*INPUT CARDS*
C   NUMBER OF TRAVERSES.
C   GAMMAS (1 VALUE/TRAVERSE)
C   BETA1,BETA2.
C   BETA3,BETA4.
C   'DATA'--MAY BE
C    BINARY, WITH  EDECK,VEL,E1,E2,E3,E4  AT EACH POINT.
C    FORMATTED, WITH FIRST 7 VALUES AT EACH POINT=
C      DATA CARD NUM(NOT USED IN COMPUTATION),EDECK,VEL,E1,E2,E3,E4.
C
C*SENSE SWITCH USE (BINARY INPUT ONLY).
C   SS0--WHEN ON, 'CALFT' ASKS FOR NUM OF POINTS TO SKIP BEFORE READING DATA.
C        (IF NUM IS NEG, NO ACTION OCCURS. IF 0, HAS EFFECT ONLY IF SS1 ON TOO.)
C     SS1--WHEN ON ALSO, SKIP BEGINS WITH NEXT CARD.
C       NOTE--SS0 SHOULD BE UP IF FIRST CALFIT DATA SET DOES NOT BEGIN AT
C                 START OF INPUT DECK, OR IF UNWANTED DATA IS BETWEEN SETS.
C             SS1 SHOULD BE UP TOO IF SUBSEQUENT SETS OCCUR IN DIFFERENT
C                 INPUT DECKS.
C   SS3--WHEN ON, TTY ASKS FOR A RESPONSE AT EACH POINT OF THE DATA SET.
C          TYPE 0 (OR EOF) TO USE POINT, ANY OTHER DIGIT TO IGNORE POINT.
C       NOTE--SS3 SHOULD BE UP IF SOME OF THE POINTS WITHIN A DATA SET ARE BAD.
C
      DIMENSION XM(4),XK(4),EO2(4),SD(4),DVDE(4),VS(4),SUMM(4)
      DIMENSION ED(100),VEL(100),WIRE(100,4),X(100)
      DIMENSION BETA(4),GAM(17)
      DIMENSION XEE(17,4),XKK(17,4),XMM(17,4)
      DIMENSION BASE(4)
      COMMON NONBL,MESS(80)
      EQUIVALENCE (X(1),ED(1))
      DATA WIREM/'WIRE'/, VELM/'VEL'/, MMESS,IBLAN/'M',' '/
      DATA XEE,XKK,XMM/204*0.0/
      DATA BASE/4*0.0/
      DATA BEE/0.92/,RADEG/0.017453293/
       CTERM(BETA,GAMMA)=(1.-BEE*(1.-SQRT(COS((BETA-GAMMA)*RADEG))))**2
  100 FORMAT(1X)
  130 FORMAT('BINARY OR FORMATTED INPUT(1=BIN,2=FOR)')
  135 FORMAT('NUMBER OF WIRES')
  137 FORMAT('NUMBER OF ITERATIONS FOR EACH CAL-FIT')
  140 FORMAT('NUMBER OF POINTS FOR GAMMA=',F5.0)
  197 FORMAT('0     GAMMA',F11.3,8X,'BETAS  ',5F15.3)
  198 FORMAT('0DV/DE'/' -----',31X,'VEL',5(6X,A4,I2,3X))
  199 FORMAT(35X,F5.0,5E15.5)
  200 FORMAT(5X,6E12.5)
  201 FORMAT('0ITERATION',I2/1X,11('-'),25X,5(9X,A4,I2))
  202 FORMAT(/30X,'EO**2',5X,5E15.5)
  203 FORMAT(30X,'K',9X,5E15.5)
  205 FORMAT(30X,A1,I9,5F15.5)
  206 FORMAT('0',29X,'M(AVGE)    ',5E15.5)
  207 FORMAT('0VELOCITIES'/1X,10('-'),21X,'VREAL',5(10X,A3,I2))
  208 FORMAT(20X,I5,6E15.5)
  209 FORMAT('0',24X,'STAND DEV',6X,5F15.5)
  210 FORMAT(I10,7F15.5)
  211 FORMAT('1',80A1/'-DATA'/' ----',13X,'ED',13X,'VEL ',5(9X,A4,I2))
  212 FORMAT('PUNCHING EO**2,K,M. 0=NO PUNCH, 1=WIRES 1 AND 2,',
     +/20X,'2=WIRES 3 AND 4, 3=WIRES 1-4.')
  213 FORMAT('NUMBER OF POINTS TO SKIP')
  214 FORMAT('VOLTAGES TO ADD TO EACH OF THE WIRE VALUES')
  215 FORMAT('COMMENT')
  221 FORMAT(4F9.5,2F9.6,' EO2,K,M/1,2 GAM#',F4.0)
  222 FORMAT(4F9.5,2F9.6,' EO2,K,M/3,4 GAM#',F4.0)
```

```
C
C*************************************************************************
C
C FIND OUT IF INPUT IS BINARY OR FORMATTED.
      WRITE(1,130)
      LLK=IDIG(1,2)
C GET NUMBER OF WIRES.
      WRITE(1,135)
      NWIRE=IDIG(1,4)
C GET NUMBER OF ITERATIONS FOR FIT.
      WRITE(1,137)
      ITER=VALUE(0,0)
C DETERMINE BASE VOLTAGE TO ADD FOR EACH WIRE.
      IF(LLK-1) 290,290,291
  290 WRITE(1,214)
      CALL GET(NWIRE,BASE(1))
  291 CONTINUE
C READ NUM OF TRAVERSES(= NUM OF GAMMAS).
      CALL READ(1,TEMP)
      ITRAV=TEMP
C READ GAMMAS FOR EACH TRAVERSE.
      CALL READ(ITRAV,GAM(1))
C READ BETAS FOR EACH WIRE.
      CALL READ(2,BETA(1))
      CALL READ(2,BETA(3))
C
C*************************************************************************
C
C *LOOP FOR EACH TRAVERSE.
      DO 500 IJJ=1,ITRAV
C IF SS0 IS ON, SKIP NUM OF PTS GIVEN BY USER, IF IN BINARY INPUT.
C   (START ON NEW CARD IF SS1 ON ALSO).
      IF(IAND(ISWIT(1),ILEFT(LLK,15))) 300,350,350
  300 WRITE(1,213)
      N=VALUE(0,0)
      IF(N) 350,310,310
  310 IF(ILEFT(ISWIT(1),1)) 320,330,330
  320 CALL BINAR(0,0,0,0)
  330 IF(N) 350,350,335
  335 DO 340 NN=1,N
      CALL BINAR(2,1,6,ED(1))
  340 CONTINUE
  350 CONTINUE
C RESET STANDARD DEVIATION SUMMATION VARIABLES.
C SET ESTIMATE OF M'S AT 0.45.   RESET MAXIMUM VELOCITY TO ZERO.
      DO 355 II=1,NWIRE
      SD(II)=0.
      XM(II)=0.45
  355 CONTINUE
      VMAX=0.0
C
C.........................................................
C GET NUM OF POINTS/TRAVERSE AND COMMENT.
      WRITE(1,140) GAM(IJJ)
      NOPTS=VALUE(0,0)
      WRITE(1,215)
      CALL TYPIN(0)
C GET DATA FOR THIS GAMMA(EDECKER,VEL,E1,E2,E3,E4)
      WRITE(3,211) MESS,(WIREM,J,J=1,NWIRE)
      WRITE(3,100)
      DO 399 K=1,NOPTS
      IF(LLK-1) 360,360,380
C (BINARY INPUT)
  360 CALL BINAR(2,1,1,ED(K))
      CALL BINAR(2,1,1,VEL(K))
      DO 365 J=1,4
      CALL BINAR(2,1,1,WWIRE)
      WIRE(K,J)=WWIRE+BASE(J)
  365 CONTINUE
C IF SS3 ON, GET DIGIT FROM KEYBOARD. IF 0 OR EOF, USE VALUE.
      IF(ILEFT(ISWIT(1),3)) 370,390,390
  370 IF(IDIG(0,9)) 390,390,360
C (FORMATTED INPUT)
  380 READ(2,200) ED(K),VEL(K),(WIRE(K,LLL),LLL=1,NWIRE)
  390 WRITE(3,210) K,ED(K),VEL(K),(WIRE(K,LL),LL=1,NWIRE)
C SQUARE ALL VOLTAGES.
      DO 395 I=1,NWIRE
  395 WIRE(K,I)=WIRE(K,I)**2
      VMAX=AMAX1(VMAX,VEL(K))
  399 CONTINUE
C PRINT OUT GAMMA AND BETA'S.
      WRITE(3,197) GAM(IJJ),(BETA(I),I=1,NWIRE)
```

```
C
C.....
C  GO THROUGH FITTING PROCEDURE 'ITER' TIMES.
      DO 499 I=1,ITER
C  COMPUTE E0**2 AND K, AS FIT OF DATA TO--
C     E2 = E02 + K * ( (VEL**M) * (1-.92*(1.-SQRT(COS(BETA-GAMMA)))**(2**M) )
      DO 410 J=1,NWIRE
      COSTM=CTERM(BETA(J),GAM(IJJ))
      ZM=XM(J)
      DO 405 K=1,NOPTS
  405 X(K)=(VEL(K)*COSTM)**ZM
      CALL LEAST(X(1),WIRE(1,J),NOPTS,E02(J),XK(J),STDEV)
      SUMM(J)=0.0
  410 CONTINUE
      WRITE(3,201) I,(WIREM,J,J=1,NWIRE)
      WRITE(3,202) (E02(J),J=1,NWIRE)
      WRITE(3,203) (XK(J),J=1,NWIRE)
      WRITE(3,100)
C  GIVEN E0**2 AND K, DETERMINE M FROM EQUATION, AND FIND AVERAGE M OVER ALL VEL
      MM=MMESS
      DO 10 J=1,NOPTS
      DO 11 L=1,NWIRE
      XM(L)=ALOG((WIRE(J,L)-E02(L))/XK(L)) /
     +      ALOG(VEL(J)*CTERM(BETA(L),GAM(IJJ)))
      SUMM(L)=SUMM(L)+XM(L)
   11 CONTINUE
      WRITE(3,205) MM,J,(XM(M),M=1,NWIRE)
      MM=IBLAN
   10 CONTINUE
      DO 12 J=1,NWIRE
      XM(J)=SUMM(J)/FLOAT(NOPTS)
   12 CONTINUE
      WRITE (3,206) (XM(M),M=1,NWIRE)
  499 CONTINUE
C
C.....
C  AFTER 'ITER'-TH ITERATION OF ABOVE PROCEDURE, DETERMINE VELOCITY.
C   ALSO DETERMINE STANDARD DEVIATION OF COMPUTED VELOCITY FROM REAL VELOCITY.
      WRITE(3,207) (VELM,J,J=1,NWIRE)
      WRITE(3,100)
      DO 18 J=1,NOPTS
      DO 19 L=1,NWIRE
      VS(L)=((WIRE(J,L)-E02(L))/XK(L))**(1./XM(L)) /
     +      CTERM(BETA(L),GAM(IJJ))
      SD(L)=(VEL(J)-VS(L))**2+SD(L)
   19 CONTINUE
      WRITE(3,208) J,VEL(J),(VS(L),L=1,NWIRE)
   18 CONTINUE
      DO 20 J=1,NWIRE
      SD(J)=SQRT(SD(J)/FLOAT(NOPTS-1))
   20 CONTINUE
      WRITE(3,209) (SD(M),M=1,NWIRE)
C
C.....
C  COMPUTE DV/DE AND PRINT.
      WRITE(3,198) (WIREM,J,J=1,NWIRE)
      WRITE(3,100)
      N=VMAX+4.99
      DO 30 I=5,N,5
      V=I
      DO 25 J=1,NWIRE
      E=SQRT(XK(J)*V**XM(J)+E02(J))
      DVDE(J)=(2.*E) / (XM(J)*XK(J)*V**(XM(J)-1.))
   25 CONTINUE
      WRITE(3,199) V,(DVDE(M),M=1,NWIRE)
   30 CONTINUE
C
C.....
C  SAVE E0**2,K,M FOR EACH WIRE.
      DO 50 J=1,NWIRE
      XEE(IJJ,J)=E02(J)
      XKK(IJJ,J)=XK(J)
      XMM(IJJ,J)=XM(J)
   50 CONTINUE
  500 CONTINUE
      WRITE(3,211)
C
C**********
C
C  PUNCH E0**2,K,M FOR WIRES 1,2 AND/OR 3,4 AT EACH GAMMA IF DESIRED.
      WRITE(1,212)
      IP=IDIG(0,3)
```

```
      IF(IP) 1000,1000,600
  600 CALL BLKCK
      IF(IP-2) 610,620,610
  610 WRITE(2,221) (XEE(I,1),XEE(I,2),XKK(I,1),XKK(I,2),
     + XMM(I,1),XMM(I,2),GAM(I),I=1,ITRAV)
      IF(IP-2) 1000,620,620
  620 WRITE(2,222) (XEE(I,3),XEE(I,4),XKK(I,3),XKK(I,4),
     + XMM(I,3),XMM(I,4),GAM(I),I=1,ITRAV)
 1000 CALL EXIT
      END)
```

```
// FOR LEAST                    COMPUTE FIT.OF DATA (X,Y) TO Y=B0+B1*X.
*NONPROCESS PROGRAM
*ONE WORD INTEGERS
*LIST SOURCE PROGRAM
**
      SUBROUTINE LEAST (X,Y,N,B0,B1,STDEV)
C LEAST COMPUTES LEAST SQUARES FIT OF N DATA POINTS (X,Y) TO THE
C EQUATION Y=B0+B1*X.
C STANDARD DEVIATION OF FITTED Y TO DATA IS RETURNED IN STDEV.
C   (WRITTEN SPRING, 1977 BY CURTISS MONROE)
      DIMENSION X(1),Y(1)
C ZERO SUMMATION VARIABLES.
      SX = 0.0
      SX2= 0.0
      SY = 0.0
      SXY= 0.0
      SERR2=0.0
C MAKE SUMMATIONS OF X, X**2, Y, X*Y.
      DO 10 I=1,N
         XI=X(I)
         YI=Y(I)
        SX=SX+XI
        SX2=SX2+XI*XI
        SY=SY+YI
        SXY=SXY+XI*YI
   10 CONTINUE
C COMPUTE B0, B1.
      B1 =  (SXY - SX*SY/N)  /  (SX2 - SX*SX/N)
      B0 =  (SY - B1*SX) / N
C MAKE SUMMATIONS FOR ERROR TERMS.
      DO 20 I=1,N
        ERR=Y(I)-B0-B1*X(I)
        SERR2=SERR2+ERR*ERR
   20 CONTINUE
C COMPUTE STANDARD DEVIATION.
      STDEV = SQRT( SERR2 / (N-1) )
C RETURN.
      RETURN
      END
```

```
// XEQ CALFT
*CCEND
```

```
C       FILE:RMSREDUC.FOR
        DIMENSION BUF(3),CONCENT_DATA(10,20)
        DIMENSION RMS_RATIO(10,20),N(10),REF_VOLT(20)
        DIMENSION NC(30),CALC_RMS_RATIO(10,50)
        DIMENSION NUM_VALUES(50),RMS_RATIO_AVE(50)
        CHARACTER*1 ANSWER,CANSWER
        CHARACTER*64 INFILE,OUTFILE,PLOTFILE
        CHARACTER*120 COMMENT
        REAL MEAS_VOLT(20)
        ANSWER='Y'
50      FORMAT('$INPUT THE NUMBER OF DATA FILES TO BE ANALYZED ')
54      FORMAT('$INPUT THE PARAMETER K [CM**3/M**2] ')
51      FORMAT('$INPUT THE FILE NAME OF THE DATA FILE #',I2)
52      FORMAT('$INPUT THE OUTPUT FILE NAME FOR THIS DATA ')
53      FORMAT(' INPUT A COMMENT STATEMENT')
55      FORMAT('$DO YOU WISH A PLOT FILE? ')
56      FORMAT('$INPUT THE NAME FOR THE PLOT FILE ')
57      FORMAT('$INPUT THE CONCENTRATION INCREMENT VALUE ')
        TYPE 50
        ACCEPT*,N_DATA_FILES
        DO 60 ITFILE=1,N_DATA_FILES
        WRITE(6,51)ITFILE
        ACCEPT 80,INFILE
80      FORMAT(A64)
        TYPE 55
        ACCEPT 82,CANSWER
82      FORMAT(A1)
        IF(CANSWER.EQ.ANSWER)THEN
        TYPE 56
        ACCEPT 80,PLOTFILE
        OPEN(UNIT=3,NAME=PLOTFILE,TYPE='NEW',ERR=301)
        ELSE
        END IF
        TYPE 52
        ACCEPT 80,OUTFILE
        OPEN(UNIT=1,NAME=OUTFILE,TYPE='NEW',ERR=302)
        TYPE 53
        ACCEPT 81,COMMENT
81      FORMAT(1X,A120)
        OPEN(UNIT=2,NAME=INFILE,READONLY,TYPE='OLD',ERR=300)
        TYPE 54
        ACCEPT*,VOL_EXTINCT
        TYPE 57
        ACCEPT*,CONC_INCREM
        NSUM=0
        MAX_NC=0
        DO 1 IA=1,10
        N(IA)=1
        DO 2 ITER=1,30
        READ(2,10) BUF
10      FORMAT(3(F10.7,5X))
        IF(BUF(1).LE.0.001) THEN
        GO TO 101
        ELSE
        IF(BUF(1).GE.9.5) THEN
        GO TO 101
        ELSE
        RMS_RATIO(IA,ITER)=BUF(1)
        REF_VOLT(ITER)=BUF(2)
        MEAS_VOLT(ITER)=BUF(3)
        CA=BUF(1)
```

```
            CB=BUF(2)
            CC=BUF(3)
            IF(ITER.EQ.1)CE=BUF(3)
            CALL SMOKE(CA,CB,CC,VOL_EXTINCT,CE,CD)
            CONCENT_DATA(IA,ITER)=CD
            N(IA)=N(IA)+1
            END IF
            END IF
2           CONTINUE
            PRINT*,N(IA)
101         CONTINUE
            NC(IA)=1
            NB=2
            CONCENT=0
            CALC_RMS_RATIO(IA,1)=1
            DO 3 ITER=2,50
            TEST_CONC=CONCENT+CONC_INCREM
            IF(NB.LE.N(IA)) THEN
            IF(TEST_CONC.LT.CONCENT_DATA(IA,NB))THEN
            CONCENT=CONCENT+CONC_INCREM
            IB=NB-1
            A=CONCENT_DATA(IA,NB)-CONCENT_DATA(IA,IB)
            B=RMS_RATIO(IA,NB)-RMS_RATIO(IA,IB)
            AB=CONCENT-CONCENT_DATA(IA,IB)
            NC(IA)=NC(IA)+1
            CALC_RMS_RATIO(IA,NC(IA))=RMS_RATIO(IA,IB)+(B*AB/A)
            MAX_NC=MAX(MAX_NC,NC(IA))
            ELSE
            NB=NB+1
            END IF
            ELSE
            GO TO 102
            END IF
3           CONTINUE
102         NSUM=NSUM+1
            IF(BUF(1).LE.0.001)GO TO 100
1           CONTINUE
100         CONTINUE
            DO 4 IA=1,MAX_NC
            SUM_RMS=0.
            NUM_VALUES(IA)=0
            DO 5 IB=1,NSUM
            IF(IA.LE.NC(IB)) THEN
            NUM_VALUES(IA)=NUM_VALUES(IA)+1
            SUM_RMS=SUM_RMS+CALC_RMS_RATIO(IB,IA)
            ELSE
            END IF
5           CONTINUE
            RMS_RATIO_AVE(IA)=SUM_RMS/NUM_VALUES(IA)
4           CONTINUE
            RMS_RATIO_AVE(1)=1.0000
            CONCENT=0.00000
30          FORMAT(' EFFECT OF OIL FOG ON HOT WIRE RMS VOLTAGE RESPONSE')
31          FORMAT(' THIS DATA IS FOR A STRAIGHT WIRE')
32          FORMAT(' THIS DATA IS FOR A SLANT WIRE')
33          FORMAT(30X,'RMS VOLTAGE RATIO')
34          FORMAT(13X,'OIL FOG')
35          FORMAT(13X,'(SMOKE)',14X,'SMOKE RMS')
36          FORMAT('+',31X,'_____________')
37          FORMAT(10X,'CONCENTRATION',9X,'NO SMOKE RMS')
45          FORMAT(9X,'[G/M**3]*10**-6')
```

```
38      FORMAT(' ',7X,'_____________________________________________')
39      FORMAT(12X,F8.3,15X,F6.3)
40      FORMAT(2(5X,E10.3))
41      FORMAT('$THE MEAN VELOCITY IS ',F4.2,' METERS PER SECOND')
42      FORMAT('$THE HOT WIRE RESISTANCE RATIO IS ',F4.2)
43      FORMAT(' ')
        READ(2,10)BUF
        WIRE_TYPE=BUF(1)
        RES_RATIO=BUF(2)
        VELOCITY=BUF(3)*(12./39.37)
        CONCENT=0
        WRITE(1,30)
        WRITE(1,43)
        IF(WIRE_TYPE.LT.1.5) THEN
        WRITE(1,31)
        ELSE
        WRITE(1,32)
        END IF
        WRITE(1,43)
        WRITE(1,42)RES_RATIO
        WRITE(1,43)
        WRITE(1,41)VELOCITY
        WRITE(1,43)
        WRITE(1,43)
        WRITE(1,33)
        WRITE(1,34)
        WRITE(1,35)
        WRITE(1,36)
        WRITE(1,37)
        WRITE(1,45)
        WRITE(1,38)
        WRITE(1,43)
        WRITE(1,39)CONCENT,RMS_RATIO_AVE(1)
        IF(CANSWER.EQ.ANSWER)WRITE(3,40)CONCENT,RMS_RATIO_AVE(1)
        DO 11 ITER=2,MAX_NC
        CONCENT=CONCENT+CONC_INCREM
        OUT_CONC=CONCENT*1000000.
        WRITE(1,39)OUT_CONC,RMS_RATIO_AVE(ITER)
        IF(CANSWER.EQ.ANSWER)WRITE(3,40)CONCENT,RMS_RATIO_AVE(ITER)
11      CONTINUE
        IF(CANSWER.EQ.ANSWER)THEN
        AFLAG=0.0000
        WRITE(3,40)AFLAG,AFLAG
        WRITE(3,40)WIRE_TYPE,RES_RATIO
        WRITE(3,40)VELOCITY,AFLAG
        WRITE(3,30)
        IF(WIRE_TYPE.LT.1.5)THEN
        WRITE(3,31)
        ELSE
        WRITE(3,32)
        END IF
        WRITE(3,42)RES_RATIO
        WRITE(3,41)VELOCITY
        CLOSE(UNIT=3,DISPOSE='SAVE')
        ELSE
        END IF
        CLOSE(UNIT=1,DISPOSE='SAVE')
60      CONTINUE
        STOP
300     TYPE 310
310     FORMAT(' ERROR IN OPENING DATA FILE')
```

```
        STOP
301     TYPE 311
311     FORMAT(' ERROR IN OPENING THE PLOT FILE')
        STOP
302     TYPE 312
312     FORMAT(' ERROR IN OPENING THE OUTPUT FILE')
        STOP
        END
```

```
FILE: SMOKE.FOR
SUBROUTINE SMOKE(CA,CB,CC,VOL_EXTINCT,CE,CD)
CD=-(LOG(CC/CE)/(2.5*10000.)
RETURN
END
```